GeoHazards

MDPI

Review

Marine geohazards of the Bay of Naples (Southern Tyrrhenian Sea, Italy): a review integrated by morpho-bathymetric and seismo-stratigraphic analysis

Gemma Aiello [1,*], Mauro Caccavale[1,2]

[1] Istituto di Scienze Marine (ISMAR), Consiglio Nazionale delle Ricerche (CNR), Sezione Secondaria di Napoli, Napoli, Italy; gemma.aiello@cnr.it
[2] Istituto Nazionale di Geofisica e Vulcanologia (INGV), Osservatorio Vesuviano (OV), Napoli, Italy; mauro.caccavale@cnr.it
* Correspondence: gemma.aiello@cnr.it

Abstract: Marine geohazards in the Bay of Naples, an eruptive region during the Late Quaternary, have been assessed based on both morpho-bathymetric and seismic data. Previously identified areas of high marine hazard with slide potential (northern Ischia slope, Naples canyons and Sorrento Peninsula-Capri slope) have been confirmed and integrated through seismo-stratigraphic analysis of selected seismic sections. We evaluated to the occurrence of important fossil submarine landslides in the stratigraphic record. Several kinds of submarine landslides have been individuated through morpho-bathymetric and seismic interpretation, including creeping, debris avalanches, debris flows, among others, often controlled by volcanic eruptions. Submarine landslides of the Naples Bay are primary geohazards in the marine and coastal areas, ascertained with significant volcanic and tsunami hazard involving the gulf. Despite previous studies on these topics, much work is still needed to compile a systematic database of the submarine landslides of the Bay of Naples, representing a future step of this research.

Keywords: submarine landslides; morpho-bathymetry; seismic stratigraphy; marine geohazards; Bay of Naples, Southern Tyrrhenian Sea.

1. Introduction

Marine geohazards are a group of underwater phenomena that can pose a threat to humans and the marine environment, with implications for coastal communities and the Blue Economy [1-2]. Forecasting is difficult, since the appearance of a marine hazard can be unexpected and infrequent. These hazards are controlled by earthquakes, volcanoes, tsunamis, and submarine mass movements [1-2].

The seabed of the Mediterranean Sea displays evidence of mass movements [1-2]. Rivers from mountains streams cause unstable sea beds. The submarine canyons trigger submarine landslides over the sea bottom of the Mediterranean Sea [3-9]. Geological processes associated with plate boundaries and active faulting cause marine hazardous events in the Mediterranean [3]. Steep and unstable continental slopes on the continental margins of the Mediterranean have been controlled by the subduction of the African plate below the Eurasian Plate. Urgeles and Camerlenghi [4] have shown that major deltaic wedges host wide submarine landslides, while tectonically active margins display small failures. Moreover, the available data highlight that submarine landslides are concentrated in the lowstand periods. Ceramicola et al. [5] have shown that the Ionian margins of Calabria and Apulia display four types of mass movements, including the mass transport complexes within intraslope basins, the isolated slide scars along open slopes, the sediment undulations genetically related to fluid migrations, and the headwalls and the sidewall scarps in the submarine canyons. These features represent important geohazards of the Calabria region. Camargo et al. [6] have proposed a review of

Citation: To be added by editorial staff during production.

Academic Editor: Firstname Lastname

Received: date
Revised: date
Accepted: date
Published: date

marine geohazards based on bibliometric searching. The obtained categories include slope failures, fluid seepages, earthquakes, tsunamis, volcanism, subsidence, bedforms, positive reliefs, negative reliefs, diapirs, faulting, and erosion. Wang and others [8] suggested using Offshore Bottom Pressure Gauges (OBPGs) around Crete Island to warn people about tsunamis early by using data assimilation. Heidarzadeh et al. [9] identified the submarine landslide as the trigger of a tsunami observed on February 2023 in the Eastern Mediterranean Sea.

The Bay of Naples, a Late Quaternary eruptive region, displays marine geohazards due to volcanism, earthquakes, submarine mass movements, fluid seepages, and anthropogenic impacts. Quaternary volcanism has significantly impacted the sea, controlling the formation of submarine volcanoes, tephra deposits [10-14] (among others), and submarine mass movements [15-18] (among others). Tephra deposits have been detected in the southern Naples Bay and in the northern Salerno Bay, represented in particular by the proximal deposits of the 79 A.D. eruption along with those of the interplinian activity at 2.7 ka B.P. [12]. These tephra correspond to stratigraphic markers interlayered within the Late Holocene marine deposits. Submarine mass movements include creep, debris flows and debris avalanches. Creeping of Holocene deposits has been recognized at the sea bottom offshore the Sarno prodelta system [10], while debris avalanche deposits have been detected offshore southern, northern and western sides of Ischia [15-16].

Tsunamis in the Bay of Naples have been suggested based on previous results [19-22]. Tinti et al. [19] simulated the tsunami triggered in the Bay of Naples by the pyroclastic flows of the Vesuvius, entering into the sea and producing an intense pressure pulse. The tsunami is small, but it moves a lot on the inside of the bay near Naples and Castellammare [19]. Tinti et al. [20] simulated the tsunami occurring at the Ischia Island, as triggered by the Ischia Debris Avalanche (IDA) [13]. These calculations determined that the eventual tsunami, triggered by a debris avalanche having the IDA dimensions, significantly involved the whole Bay of Naples, with the highest waves at Ischia, Capri and Sorrento Peninsula [20]. Selva et al. [21] analyzed the natural hazards of Ischia, developing their interpretative framework. The obtained results have shown the important role of the volcanic hazards (eruptions, tephra), as well as the non-volcanic ones (earthquakes, landslides, and tsunamis). Quantitative hazards have not still evaluated and the block resurgence of Ischia has a fundamental role in their calculation. Grezio et al. [22] have suggested that the first-order tsunami hazard results have the highest probabilities exceeding levels of about 1–1.5 m in 50 years and occur at the Naples town, Campi Flegrei, and Ischia.

In this paper, we discuss the marine geohazards of the Bay of Naples, based on both the literature review of the data existing on the area and on the morpho-bathymetric and seismic interpretation of marine geohazards, previously identified [23-24], in the northern slope of Ischia, Naples canyons, and southern slope of Sorrento Peninsula-Capri Island structural elongment. Based on seismic interpretation, we provide further data and constraints on the occurrence of important fossil submarine landslides in the Naples Bay, highlighting that different types of submarine landslides can be detected in this complex volcanic area. Figure 1 shows the geologic sketch map of the Bay of Naples and of the surrounding emerged areas., while Figure 2 displays a Digital Elevation Model of the Naples Bay, with the location of the three study areas, indicated as the sectors having a high marine hazard in the Naples Bay [23-24].

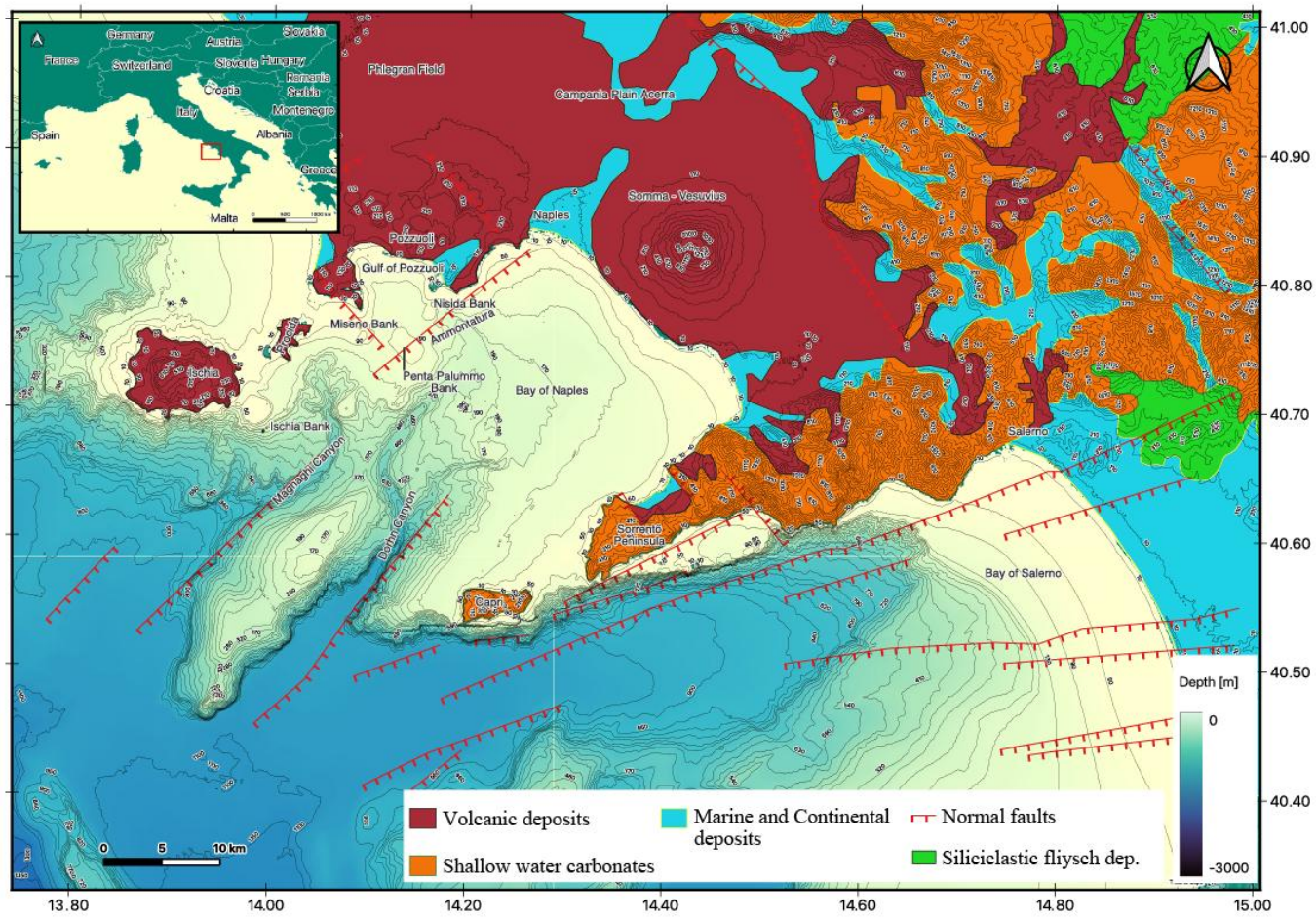

Figure 1. Geologic sketch map of the Bay of Naples and of the surrounding emerged areas.

2. Geological setting

The Bay of Naples represents a half-graben on the continental margin, produced by broad extension alongside the Apenninic chain [25] (Figure 1). The geological framework of this basin is characterized by alternating structural highs and lows in a transtensional tectonic setting [26-28]. In the Campania country, Quaternary basin deposits overlie the westerly Apenninic tectono-stratigraphic sequences, arising from the continuation towards the offshore of the matching units outcropping in the marginal zone of the southern Apennines [29-30]. These tectonic assemblages compose the basement of the littoral basins and consist of flysch deposits or of Meso–Cenozoic carbonates (Figure 1).

A structural high with a WSW-ENE trend is found on the Sorrento Peninsula, sandwiched between two half-grabens, the Bay of Naples and the Bay of Salerno (Figure 1) [31]. Its structural framework is characterized by NW dipping blocks, resulting from tectonic phases ranging in age from the Late Miocene to the Quaternary [31].

Mesozoic carbonates appear in the peninsula and are overlain by a transgressive Miocene sequence and, then, by breccias and pyroclastic rocks, Pleistocene to Holocene in age (Figure 1). The 79 A.D. pyroclastic unit overlies the Mesozoic rocks or eruptive units of the Middle-Late Pleistocene. Between 18 ky ago and 79 A.D. the headland did not display appreciable pyroclastic deposits, because, during this time frame, the Plinian eruptions were propagated towards the east and north-east [31-32].

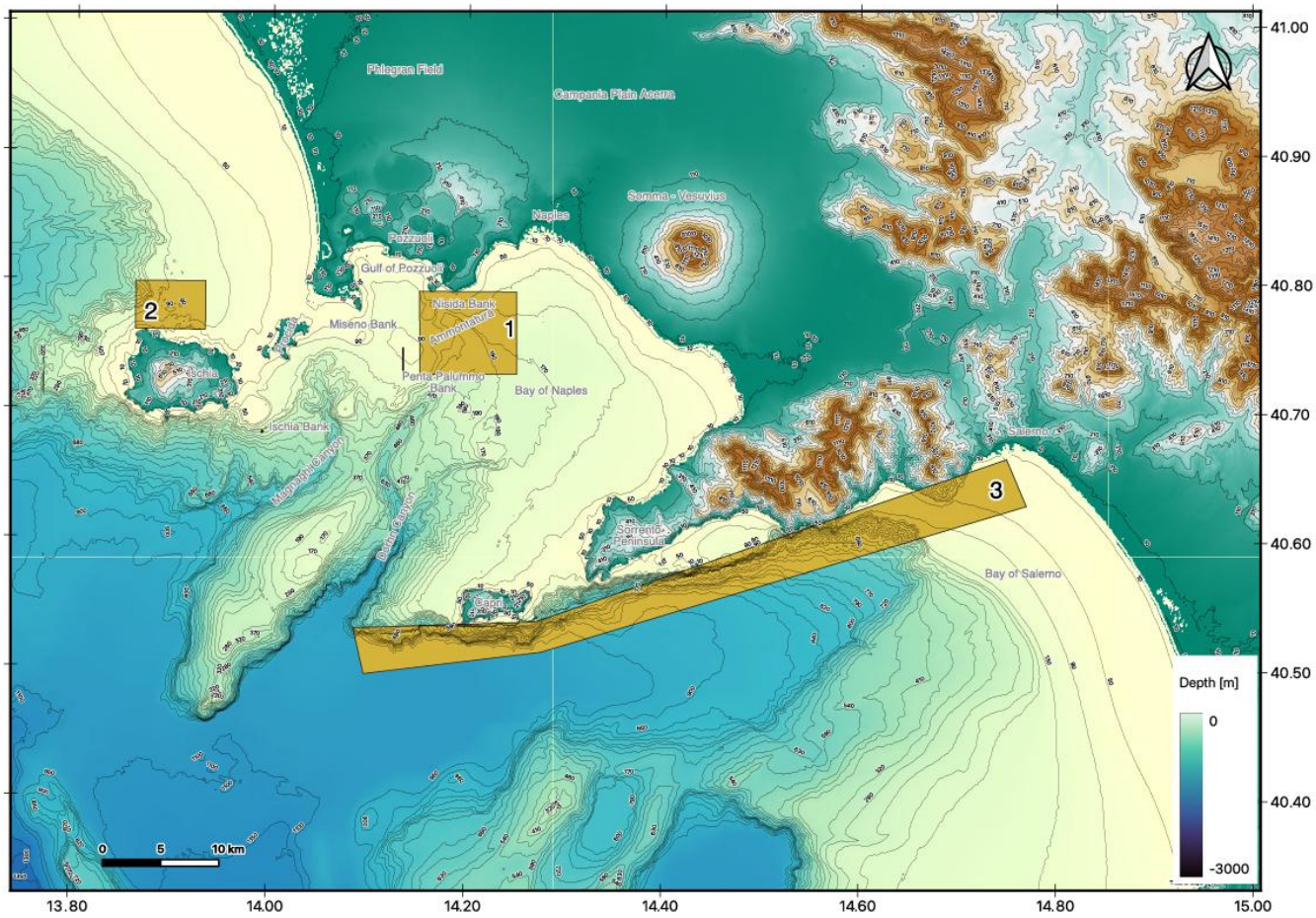

Figure 2. Digital Elevation Model of the Naples Bay showing the location of study areas (1: Ammontatura slope basin and northern branch of the Dohrn canyon; 2: northern Ischia debris avalanche deposits; 3: southern slope of the Sorrento Peninsula).

Ischia Island has been deeply studied, regarding the debris avalanche deposits, both offshore [33-37] and onshore (Figure 3, inset a [37]). Seven debris avalanches surround the Epomeo Mt, showing a close relationship with the corresponding deposits on the continental shelf [38] (Figure 3, inset b).

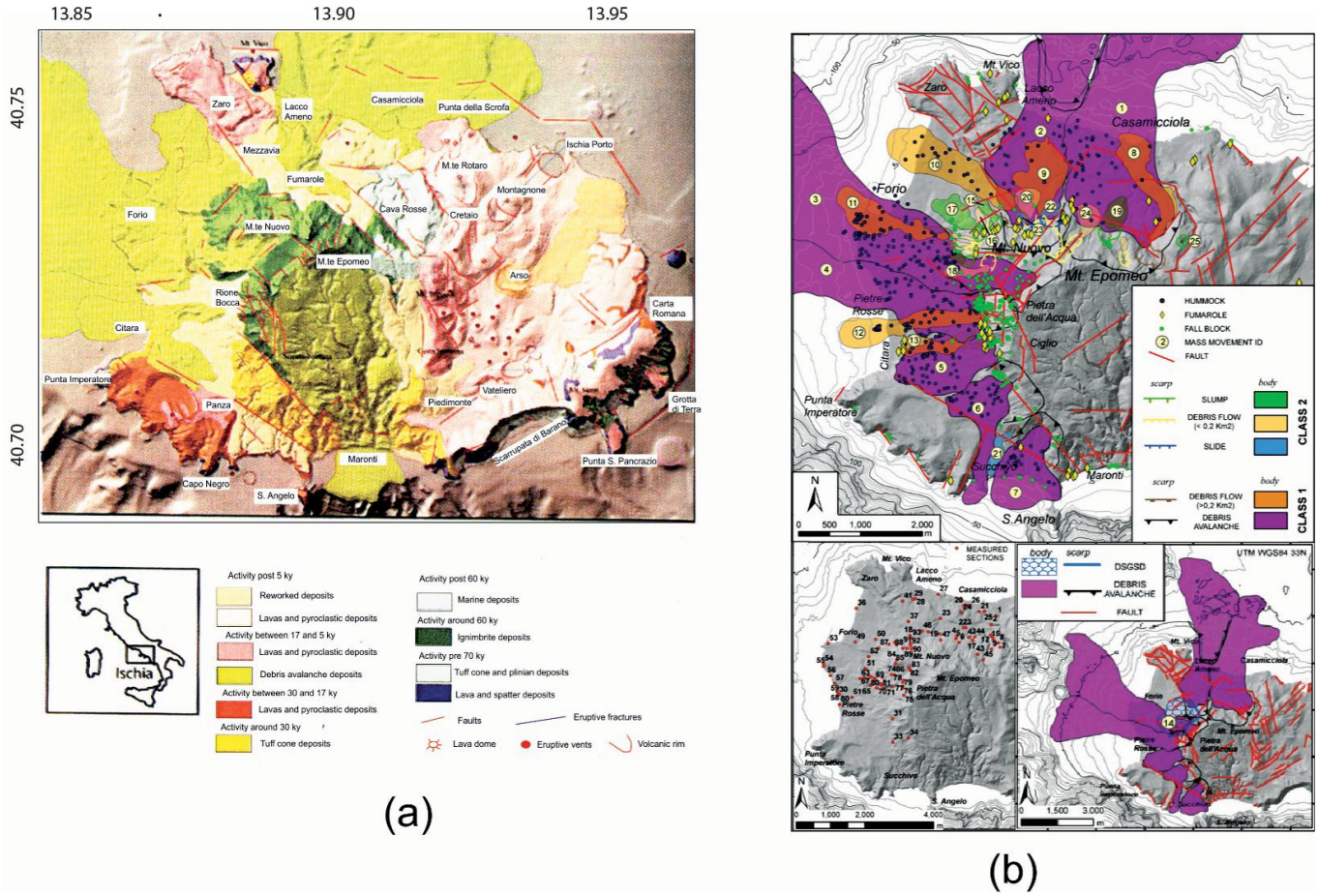

Figure 3. (a) Geologic sketch map of Ischia (modified after Sbrana et al.) [37]. (b) Onshore and offshore extension of the Epomeo Mt. gravitational landforms and offshore extension of the debris avalanche deposits (modified after Della Seta et al.) [38].

3. Materials and methods

Literature review has been carried out for the identification of marine hazards of the Naples Bay, regarding the earthquakes, submarine landslides, tephra deposits, pyroclastic density currents (PDC), and tsunamis. The geophysical dataset consists of Multibeam and seismic data of the Naples Bay and of the Salerno Valley. Curiosity driven research has been carried out for the Salerno Valley and the southern slope of the Sorrento Peninsula (Sister II oceanographic cruise, CNR ISMAR, Naples, Italy).

Detailed DEMs and bathymetric profiles have been constructed by using the Global Mapper software, TRIAL version (https://globalmapper.it/download.php). Multichannel seismic profiles (GRNA35; oceanographic cruise GMS00_05; CNR ISMAR, Naples, Italy) and Sparker seismic profiles recorded for the marine geological survey of the Ischia Island at the 1: 10.000 scale have been interpreted. Multichannel seismic acquisition was carried out at constant distance interval of 6.25 m, with a receiver interval of 6.25 m, a minimum offset of 130 m and a fold of 1200%. The data recorded by the hydrophones have been acquired using the Stratavisor NX (Geometrics Inc.), recording 24 channels. Sparker seismic acquisition was performed using a Multitip sparker system (SAM96 model), whose technical characteristics include short pulse lengths and increasing peak pressure. This Sparker system generated 200 J in the 200–2,000 frequency range. Seismic profiles have been interpreted by using the CorelDraw graphic suite, version 17.0 (https://www.coreldraw.com/it/).

4. Results

4.1. Literature review

4.1.1. Earthquakes

Vesuvius, Campi Flegrei, Ischia and Procida are hazardous volcanoes, where seismicity occurred in recent times. In recent years, the earthquakes have been mainly controlled by the Campi Flegrei bradyseism. The eruption of the caldera has been happening for at least 10 million years. The Phlegrean caldera reactivation is believed to be associated with volcanism, ground deformations, and seismicity. In the uplifted section of the caldera, the volcanic edifices prevail, achieving both long-term deformation, that is to say the resurgence, and short-term deformation, that is to say the bradyseism. Two main bradyseismic crises are known between 1969–1972 and 1982–1984.

Table 1 shows that significant earthquakes occurred in the Campi Flegrei and Naples Bay in recent years (https://terremoti.ingv.it/events). The earthquakes are listed by decreasing magnitude and represent a main geohazard in the Naples area. During the last year (2023) 572 earthquakes occurred at Campi Flegrei and Vesuvius based on the INGV catalogue. The most significant ones (magnitude between 3 and 4) have been reported in Table 1. The earthquake of Casamicciola (Ischia) on 21/8/2017 has also been reported, due to the intense destructive effects.

Table 1. Earthquakes in the Bay of Naples (https://terremoti.ingv.it/events)

Time	Magnitude (Mw)	Location	Depth	Latitude	Longitude
27/9/2023	4.2	Campi Flegrei	3 km	40°82′	14°16′
2/10/2023	4.0	Campi Flegrei	3 km	40°83′	14°15′
21/8/2017	3.9	Casamicciola (Ischia)	2 km	40°74′	13°90′
7/9/2023	3.8	Campi Flegrei	3 km	40°83′	14°15′
16/10/2023	3.6	Campi Flegrei	2 km	40°83′	14°14′
11/6/2023	3.6	Campi Flegrei	3 km	40°83′	14°11′
18/8/2023	3.6	Campi Flegrei	2 km	40°83′	14°14′
8/5/2023	3.4	Campi Flegrei	3 km	40°83′	14°14′
22/9/2023	3.0	Campi Flegrei	1 km	40°83′	14°14′
23/11/2023	3.1	Campi Flegrei	3 km	40°83′	14°14′
17/2/2024	3.0	Campi Flegrei	3 km	40°84′	14°12′

Campi Flegrei earthquakes are genetically related with bradyseism. A 4.3 magnitude earthquake hit Campi Flegrei, on 27 September 2023 (Table 1). It was the region's longest-lasting quake in 40 years, and it was a component of a seismic sequence that has been reverberating Campi Flegrei for a couple of weeks. To better understand these trends, Kilburn et al. [39] constructed a model to keep track of the evolution from an

elastic state to an inelastic one, where rocks begin to fracture more and more and breaking originates beneath the faults. In this scenario, the frequency of local earthquakes is directly related to the rate of ground deformation. In the first instances, the ground deformation brings about a few earthquakes, but as the stress increases in the crust, the same quantity of ground deformation, with time, quickens the frequency of earthquakes [39]. To the extent that the unrest has affected the geometry of Campi Flegrei's crust, the reported findings introduced data for forecasting the volcano's likelihood to erupt or to subside prior to eruption [39].

The destructive faults located in the Ischia Island controlled the Casamicciola earthquake occurred in 2017. De Novellis et al. [40] provided explanation of the earthquake based on integrated geophysical study aimed at reconstructing the focal mechanisms of the Casamicciola earthquake [40]. The obtained results revealed an E-W striking, south dipping normal fault, which is compatible with the rheological stratification of the crust at Ischia.

4.1.2. Submarine landslides

In the Naples Bay the submarine landslides are an important marine geohazard. Significant slides have been detected both at Ischia and in the central Naples Bay, in the Dohrn and Magnaghi canyons, while creeping of the sea bottom occurs offshore the Sarno river mouth towards the Vesuvius coastline. The N and W onshore sectors of Ischia are affected by debris avalanches [38], as well as the offshore, where hummocky deposits have been identified [33-37]. Onshore, they include a debris avalanche detached from the western flank of the Epomeo Mt. and a deep seated gravitational deformation involving the Monte Nuovo [38]. Between the debris avalanches of Ischia, the largest one is the Ischia Debris Avalanche (IDA) [15].

Significant submarine slides occur in the Dohrn canyon system, where slide scars do not correspond with adjacent slide deposits, which have been probably reworked and removed by sea bottom currents [18, 24, 41]. During the Late Quaternary, submarine slides mainly involved both the canyon's heads, being respectively double regressive (Dohrn) and triple regressive (Magnaghi). In this area, the geological evolution of submarine slides has been explained according to the three-stage model of Pratson and Coakley [42] for submarine canyon evolution [43]. This approach is centered on the modification of the slope failures in a canyon with a retreating head, receding upwards on the slope along the pre-canyon channels, as dictated by the retrogressive slides modulated by strong volcaniclastic input. The first phase, corresponding to the carving of the pre-canyon channels, happened in a time interval ranging between 37 ky B.P. (eruption of the Campanian Ignimbrite) and 15 ky B.P. (eruption of the Neapolitan Yellow Tuff). The second phase, corresponding to the canyon development through slope failures, happened later than 15 ky B.P. (eruption of the Neapolitan Yellow Tuff) [43]. The third stage, corresponding to the individuation of the canyon retrogressive heads, is older than the growth of the Nisida volcanic bank (Naples offshore), physically interrupting the Dohrn western branch (4.8-3.8 ky B.P.) [43]. Figure 4 shows the high-slope map of the Naples Bay, previously constructed [24], identifying the areas prone to slide, having gradients major than 10°.

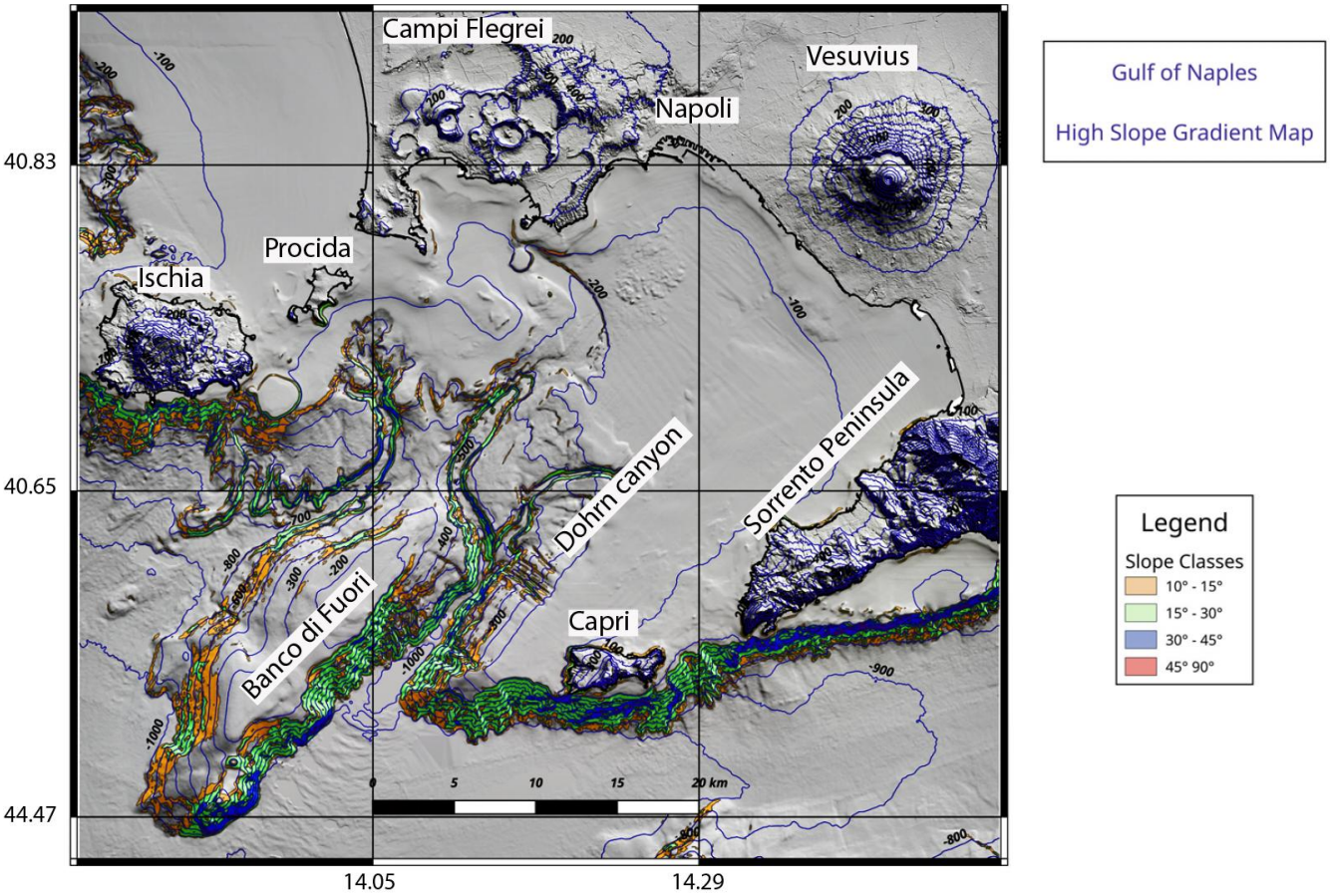

Figure 4. High-slope map of the Naples Bay, showing marine areas potentially prone to slide (modified after Aiello and Sacchi [24]).

4.1.3. Marine tephras

Marine sediment cores enclosing tephra provide reliable datasets for volcanic and marine hazards [44]. Satow et al. [44] highlighted that the marine sediment cores give detailed information on long-term hazard assessment, being archives of volcanic activity. They include ash (tephra) deposits, cryptotephra deposits, pyroclastic density current (PDC) deposits, and reworked volcaniclastic deposits, giving detailed geologic and volcanologic information on marine hazards.

Many studies have been carried out in the Bay of Naples, regarding the marine tephra layers, providing information on the marine and volcanic hazards, both at Ischia [45-50] and on the Naples continental shelf [12; 51-53]. The reconstructed stratigraphic model provides improved estimates of future eruption hazards, such as plume height and the total volume of eruptive material.

Brown et al. [45] established the general stratigraphic setting of the south-eastern Ischia tephra. De Alteriis et al. [46] recognized two collapse events of the IDA, including the Ischia submarine debris avalanche/debris flow (DA/DF), dated between ~ 3 ka B.P. and 2.4 ka B.P. and a former, pre-Holocene, DA/DF older than 23 cal ka B.P. De Vita et al. [47] examined the impact of the Ischia Porto tephra, consisting of a poorly dispersed pyroclastic deposit, on the Greek settlements of Ischia, based on recent excavations on S. Pietro Hill, eastwards of Ischia harbor.

Tomlinson et al. [48] analyzed the distal tephra layers of Ischia, spanning a time interval between 104-39 ky B.P., which yielded proximal-distal trends for a broad spectrum of eruptions. Primerano et al. [50] reconstructed the Cretaio tephra fallout dispersal, which is larger than previously known, and extends from the Naples Bay to the middle of

the Tyrrhenian Sea, at the latitudes of the Cilento Promontory [62], as shown by the map of the ground deposit isomass lines (Figure 5a).

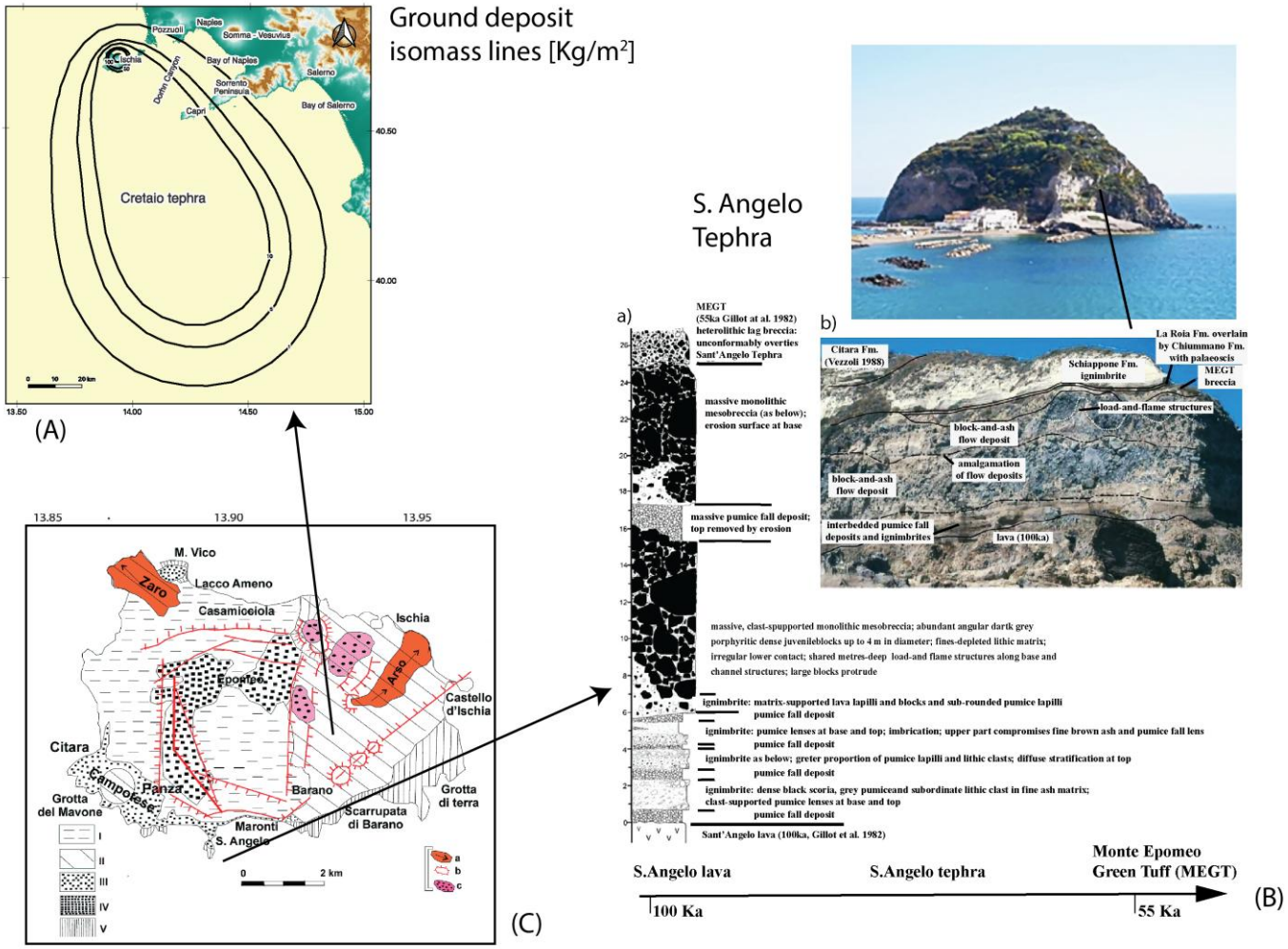

Figure 5. (a) Ground deposit isomass lines (kg/m²) on domain covered by Cretaio tephra (Tyrrhenian Sea; modified after Primerano et al. [50]. (b) The S. Angelo tephra of Ischia (modified after Brown et al. [45]). (c) location of the Cretaio and S. Angelo tephra superimposed on the geological map of Ischia.

In the Bay of Naples marine tephra deposits have constrained the eruption magnitude and frequency in the area, as well as the distribution of pyroclastic deposits associated with the most recent activity of Vesuvius [51-53], improving the knowledge on marine hazards.

Core data have shown the 79 AD Vesuvius tephra, interstratified in the Quaternary marine succession (Figure 6) [51-53], has a thickness ranging between 90 and 40 cm next to the Sarno Plain (C81, C82, C4) and 10 cm next to the shelf margin of Naples Bay (C69). Figure 6 shows that the tephra is located below older Quaternary marine deposits.

In the proximal areas the tephra deposits consist of coarse-to-medium grained sands and gravels. In the distal areas it consists of sandy silts with fine-grained lithic and bioclastic components [43; 51-53] (Figure 6).

4.1.4. Pyroclastic density currents

Pyroclastic density currents (PDCs) are the most damaging phenomena that arise during explosive eruptions. These flows of ash and debris are spreading at travel speeds of hundreds of meters per second, reaching many tens to hundreds of kilometers from

the starting point. These currents tend to be erratic, and as they move forward, they transform in type between dense, clastic flows and dilute ash- and gas-rich surges, capable of dispersing from the main body of the flow and overthrowing topography.

PDCs deposits are widespread in the Bay of Naples during the Late Quaternary. At Ischia, forty-seven eruptions occurred during the last 10 ky, generating PDCs deposits, mainly composed of ash surges [54]. PDCs deposits of Ischia were mainly deposited in the eastern portion of the island and the corresponding hazards have been discussed by Alberico et al. [55], who constructed maps of the frequency of the PDCs invasion.

All the Plinian eruptions of Vesuvius have emplaced important pyroclastic density current (PDCs) deposits. The correlation of the seismic unit with the fallout deposits representing the base of the AD 79 eruption has been made checking the dispersions of these PDCs, corresponding with the seismic unit, on isopach maps of the "Pomici di Mercato" and "Pomici di Avellino" deposits, available in the volcanological literature of the area [56-61].

In addition, the PDCs deposits of the "Pomici di Mercato" are roughly concentrated along the northern flanks of Mt. Somma, suggesting that the caldera was established in a geographic location that is comparable to today's Vesuvius edifice. However, the location of the outcrops of the "Pomici di Mercato" in correspondence with the Sebeto Plain and along the Tyrrhenian coastline well fits with the location of a seismic unit located offshore, and identified on seismic profiles [62]. Instead, the PCDs deposits of the "Pomici di Avellino" have a maximum thickness in the western area of the volcano. An important new seismic unit, recognized offshore the Somma-Vesuvius [67] has been correlated with the fallout deposits representing the base of the AD 79 eruption of the Vesuvius volcanic sequence [56-61].

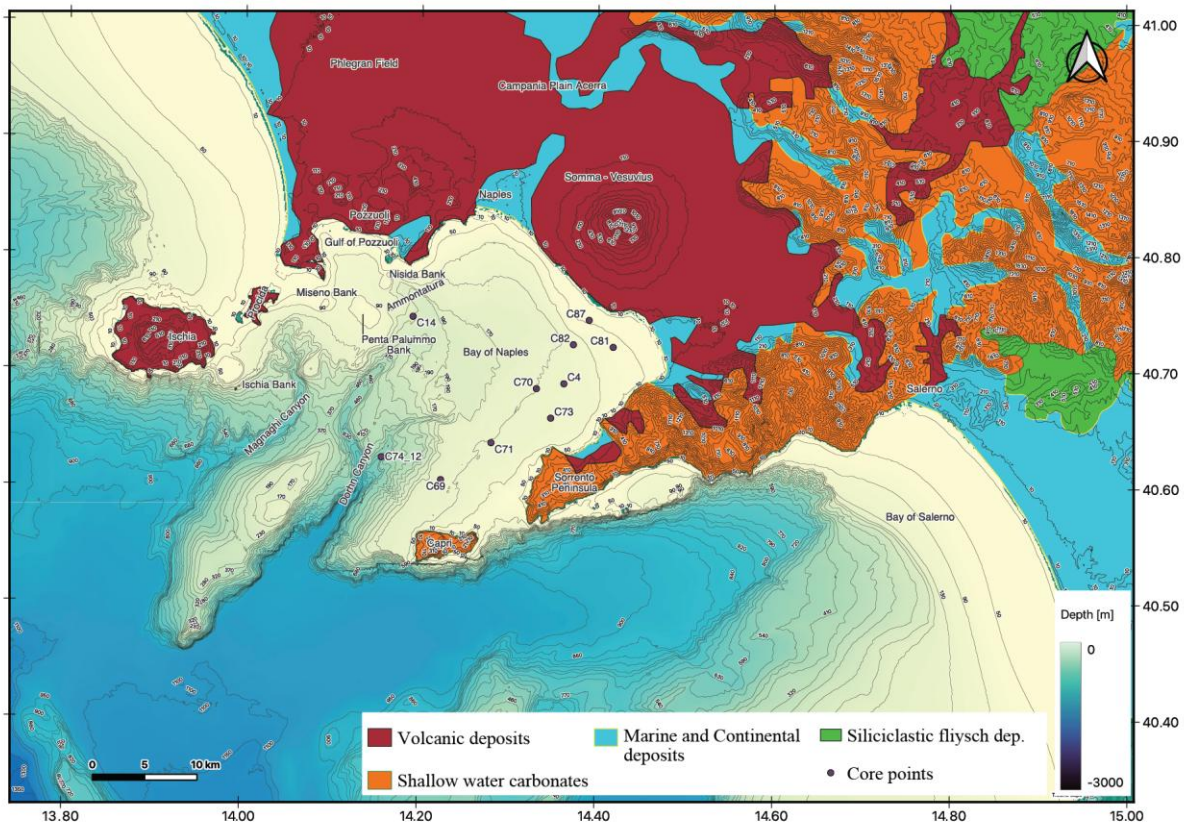
Phlegran Field
Campania Plain Acerra
Somma - Vesuvius
Naples
Pozzuoli
Gulf of Pozzuoli
Nisida Bank
Miseno Bank
Ammonatura
Ischia
Penta Palummo Bank
Bay of Naples
Ischia Bank
Magnaghi Canyon
Dohrn Canyon
Sorrento Peninsula
Capri
Salerno
Bay of Salerno
C87
C82
C81
C14
C70
C4
C73
C71
C74
C12
C69
Depth [m]
0
-3000
Volcanic deposits
Marine and Continental deposits
Siliciclastic fliysch dep.
Shallow water carbonates
Core points
0 5 10 km
41.00
40.90
40.80
40.70
40.60
40.50
40.40
13.80
14.00
14.20
14.40
14.60
14.80
15.00

(A)

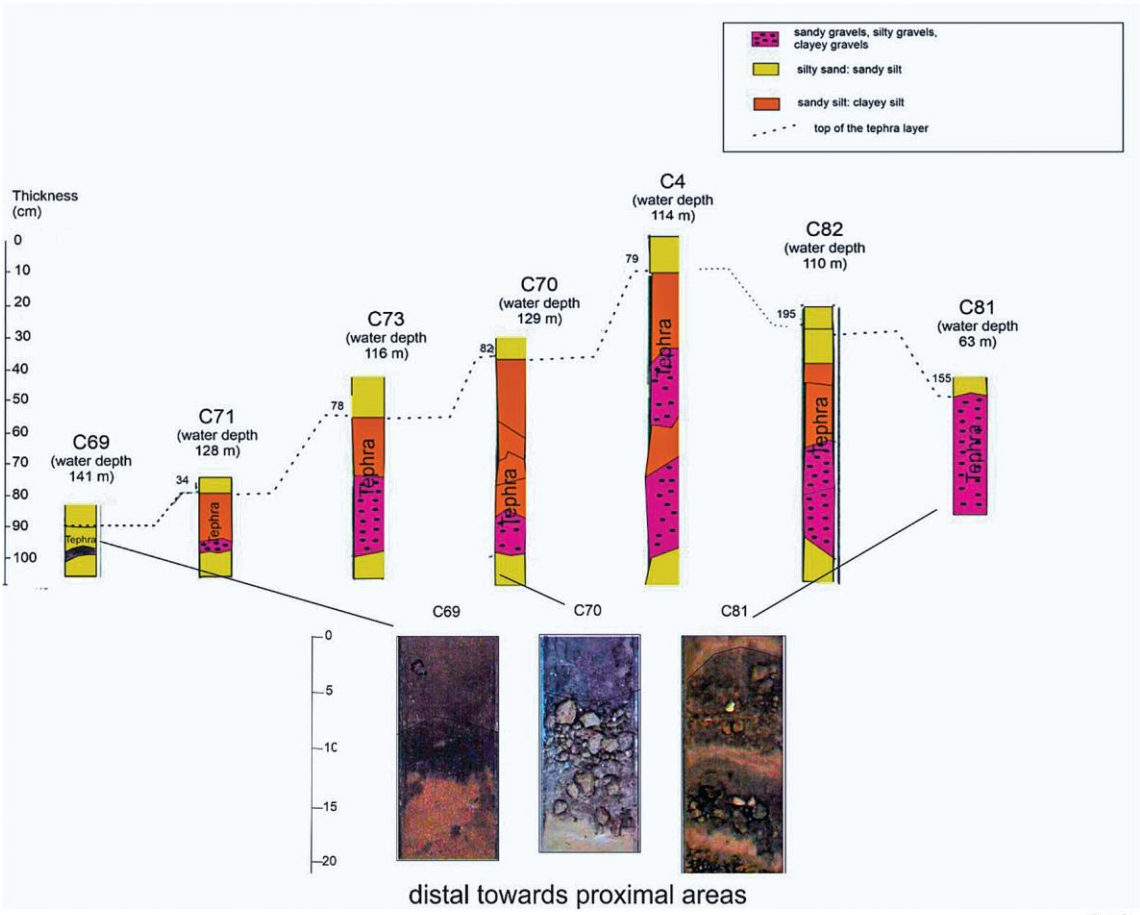
sandy gravels, silty gravels, clayey gravels
silty sand: sandy silt
sandy silt: clayey silt
top of the tephra layer
Thickness (cm)
0
10
20
30
40
50
60
70
80
90
100
C69
(water depth 141 m)
C71
(water depth 128 m)
C73
(water depth 116 m)
C70
(water depth 129 m)
C4
(water depth 114 m)
C82
(water depth 110 m)
C81
(water depth 63 m)
34
78
82
79
195
155
Tephra
C69
C70
C81
0
5
10
15
20
distal towards proximal areas

(B)

Figure 6. (a) Location map of the cores showing marine tephra in the Naples Bay (modified after Aiello and Caccavale [43]. (b) Sketch stratigraphic section of the C69,C71, C73, C70, C4, C82, C81 cores [51-53],where the top of the tephra layer has been reported and detailed core photographs showing the passage from distal (fine-grained) to proximal (coarse-grained) areas.

Pyroclastic flows can flow into the seawater, propagate, and reach elevated temperature levels for vast regions underwater because of the discovery of ignimbrites in marine sedimentary formations [63-68]. Sparks et al. [64] reported that the underwater habitats are more ideally suited to the welding process than many terrestrial locations. At relatively small water depths, when water and hot ash come into contact at the boundary of a flow, they can spark an explosion and cause some strong flows to be destroyed. The prerequisites for the escape of a pyroclastic flow into deep water usually involve steep slopes and a huge rate of flow. Trofimovs et al. [65] observed the behavior of pyroclastic flows entering the sea, when 90% of the total material was deposited into the submarine settings. When the main flow enters into the sea, phreatic explosions occur and a surge cloud originates. The coarse-grained components of the flow are deposited in proximal environments, while the fine-grained components are elutriated in the upper part of the flow, forming a turbidity current. Di Capua and Groppelli [66] showed that the PDCs that interact with the water usually experience physical alteration, producing flow dispersal and reorganization in cold, water-supported turbidites. In any case, the reliability of primary volcanic structures has been fully attested in shallow waters. A geological survey and laboratory analysis concluded that the granular flow-dominated scenarios describe the most suitable flow mechanism conditions of the pyroclastic flows in the Val d'Aveto Formation [66]. Clare et al. [67] showed that the immediate release of huge quantities of erupted solids onto steep undersea slopes created fast seafloor flows. These density currents were more rapid than those brought on by earthquakes, floods, or storms [79]. Maeno and Imamura [68] highlighted that, for the pyroclastic flow hypothesis, two sorts of two-layer shallow water simulations, dense- and light-type models, were employed owing to divergent launch scenarios in the Krakatau eruption of Indonesia. It is worth noting that this kind of two-dimensional models have not still applied to the PDCs of the Bay of Naples, and further work is required for the volcanologists.

Milia et al. [63] explained the effects of the pyroclastic fluxes in the Naples Bay. In particular, these authors constructed a map showing the main pyroclastic fluxes entering the sea in the Naples Bay (Figure 7). These fluxes have been represented by the isopachs of the AD 79 pumice fall deposits and pyroclastic flow deposits (Figure 7). An undersea volcaniclastic fan that has its roots from the AD 79 eruption of the Vesuvius stands for the resiliency of the PDCs that fossilized the Roman village of Herculaneum (Pompei).This fan represents a well-documented stratigraphic record of PDCs erupted on the continental platform in a shallow water setting, as controlled by syn-depositional reworking by wave action.

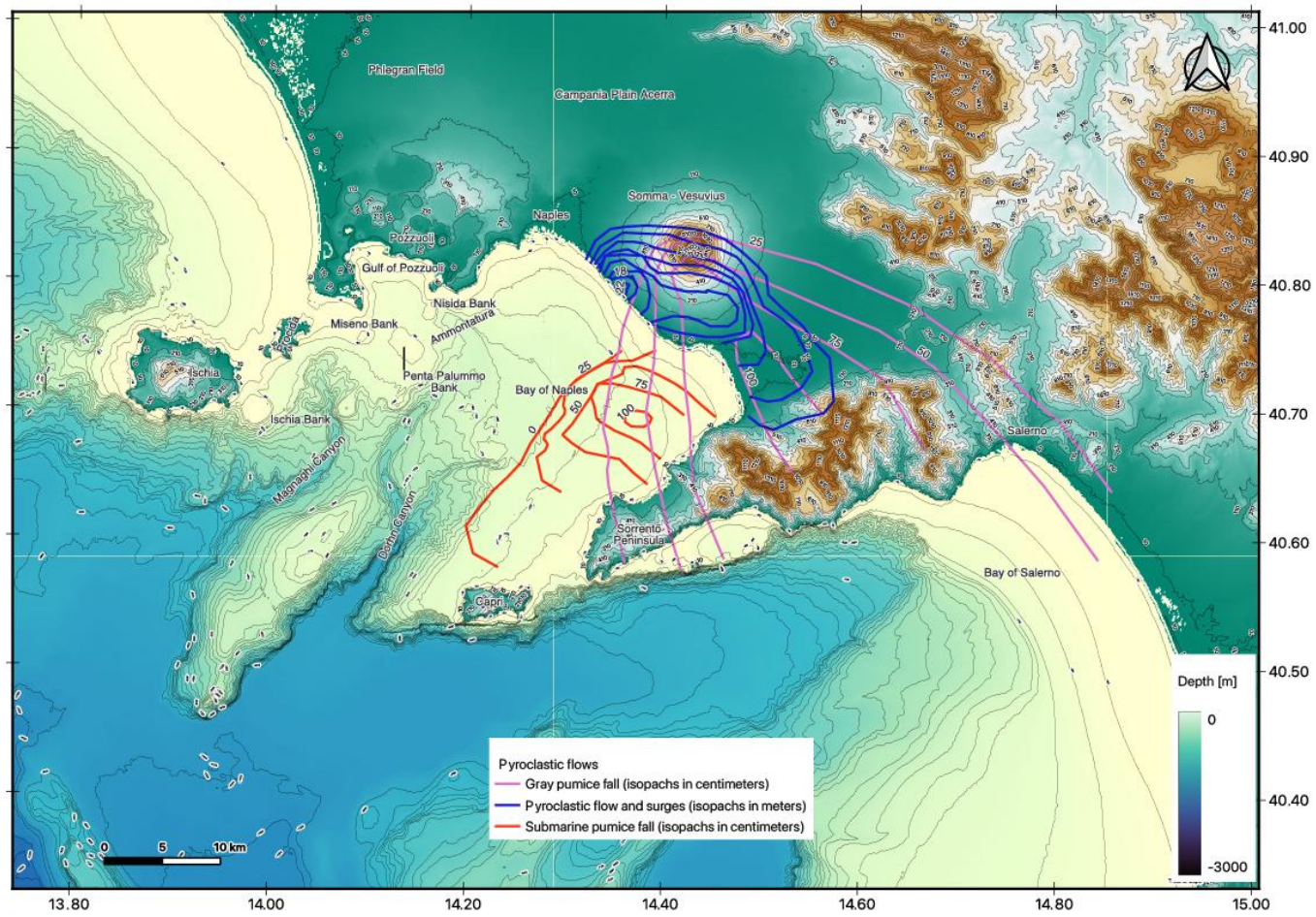

Figure 7. Pyroclastic flows in the Naples Bay (modified after Milia et al. [63].

4.1.5. Tsunamis

In the Naples Bay tsunamis constitute a severe geohazard, due to their close relationships with the volcanic eruptions, earthquakes and submarine landslides [19-22; 69-73]. Historical tsunamis have also been documented, including the 1343 tsunami, affecting Tyrrhenian Sea, including the Bay of Naples [71, 73]. This tsunami destroyed many harbors including Amalfi and has been documented by historical sources [73]. This event could be genetically related to the flank collapse of the Stromboli volcano [71]. To analyze the proportions of tsunamis caused by different reasons in the Naples Bay is still a complicated matter and requires further studies. For the models known in previous literature, only numerical simulations have been carried out and explanation of different proportions of tsunamis is not certain. Tinti et al. [19] studied the triggering of tsunami and its propagation in the Naples Bay controlled by Vesuvius pyroclastic flows. A finite-element model has been used for the simulation, showing that the oscillations are larger in the gulf and more negligible proceeding basinwards (Figure 8, inset a) [19]. Di Fiore et al. [41] evaluated the tsunami and wave-run up in the Dohrn canyon, showing a detachment area, about 415 m across at water depths ranging between −250 m and −370 m (Figure 8, inset b) [41]. The obtained results have shown that the amplitude wave run-up expressed in terms of depth of seafloor percentage, varies from 0 to 2.5 % and the wave height amplitude corresponds to 5−6 m (Figure 8, inset b) [41]. Tinti et al. [20] simulated the tsunami triggered by the IDA [13], showing that on Ischia the wave amplitudes exceed 40 m, while Capri is reached by the wave after about 8 min, with relevant waves (Figure 8, inset c) [20]. Alberico et al. [69] analyzed the tsunami vulnerability of the city of Naples, which is composed of the water vulnerability, and structural vulnerability. A high structural vulnerability characterizes the Chiaia area close to the

shoreline and the eastern sector of the Sebeto-Volla plain, whereas in the western sector this area is controlled by the presence of a 70 m structural high, preventing the onshore propagation of the tsunami wave.

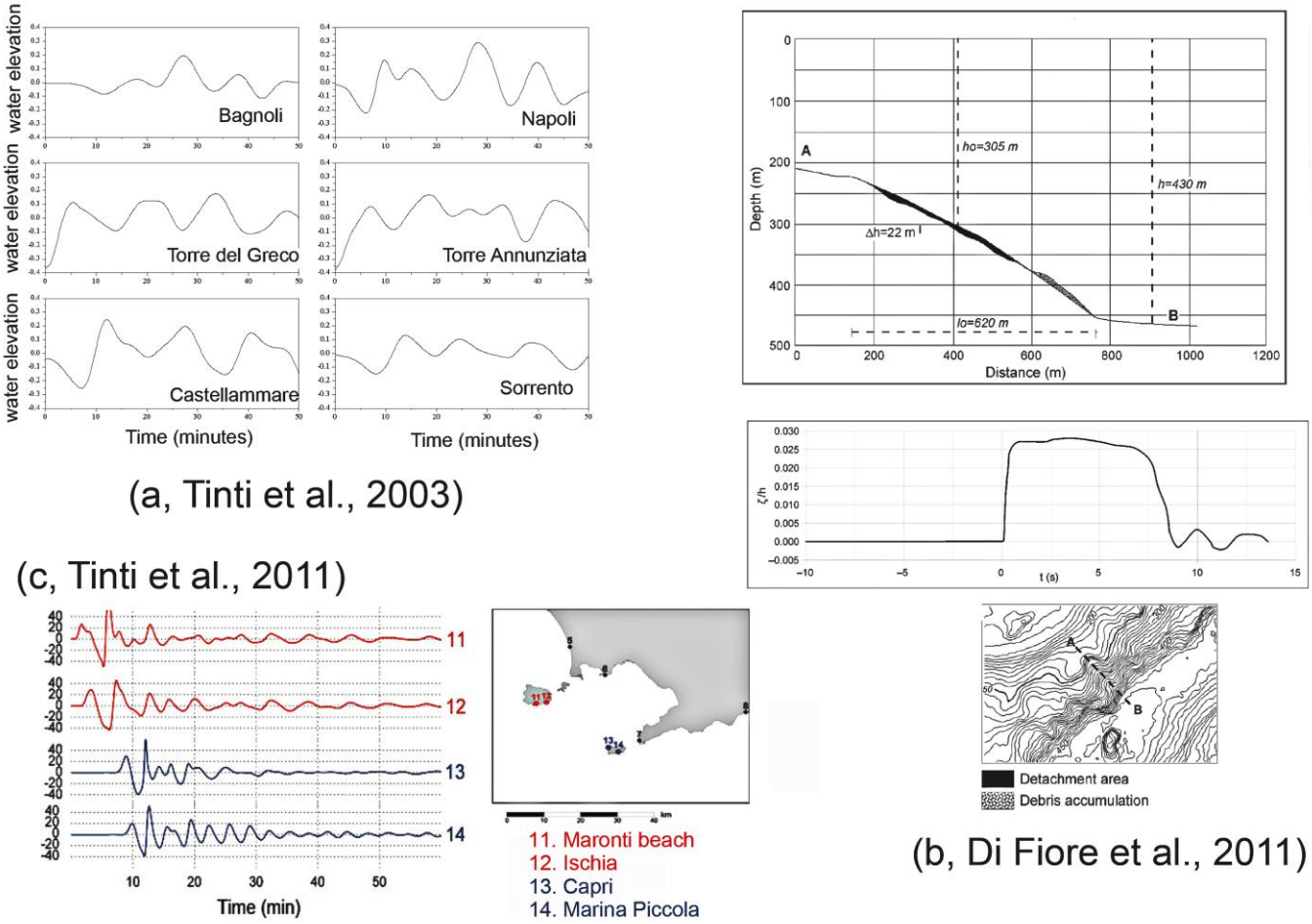

Figure 8. Mareograms related to tsunami in the Naples Bay (a, modified after Tinti et al. [19], Di Fiore et al. [41]) and Ischia (c, modified after Tinti et al. [20])

4.2. Morpho-bathymetric and seismo-stratigraphic analysis

4.2.1. Ammontatura slope basin

Detailed Digital Terrain Model (DTM) and bathymetric profiles are herein revised (Figure 9). The center of the Bay of Naples is outlined by the Ammontatura channel, which is the seabed physiographic expression of the Ammontatura slope basin. The channel is 2.5 km wide and 20-40 m deep. DTM and bathymetric profiles have displayed that this channel shows a curved form, a smooth thalweg, and unbalanced scarps. This channel splits the "Banco della Montagna" feature from the volcanic brinks of the Campi Flegrei. Bathymetric profiles demonstrate that the western slope of the Ammontatura channel is broadly more precipitous than the eastern one. In its northernmost part, the pivot of the channel flexes towards the north-west and shortly aborts N of the Nisida Bank (Figure 9).

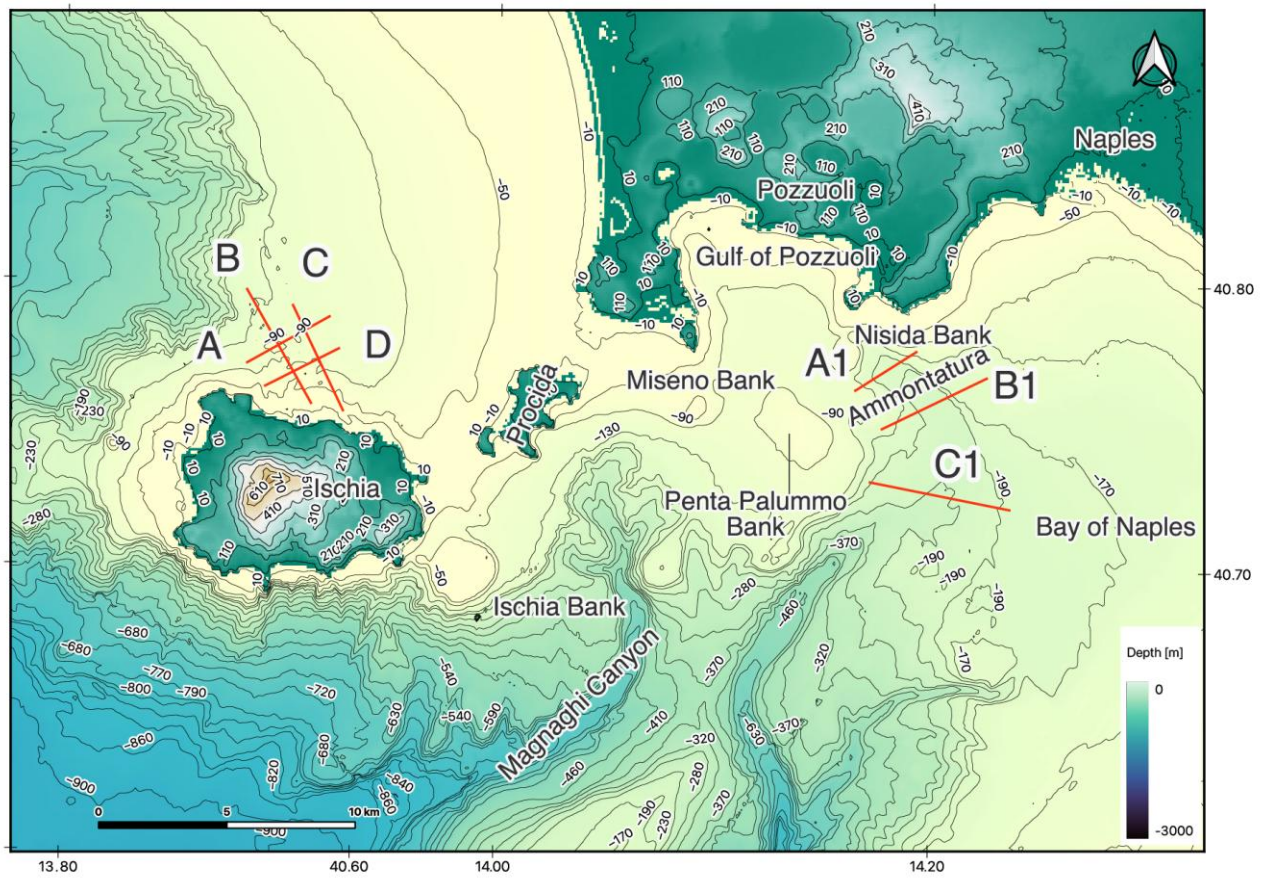
Naples
Pozzuoli
Gulf of Pozzuoli
Nisida Bank
Miseno Bank
Procida
Ischia
Penta Palummo Bank
Bay of Naples
Ischia Bank
Magnaghi Canyon
A
B
C
D
A1
B1
C1
Ammontatura
Depth [m]
0
-3000
40.80
40.70
13.80
40.60
14.00
14.20
0
5
10 km

381

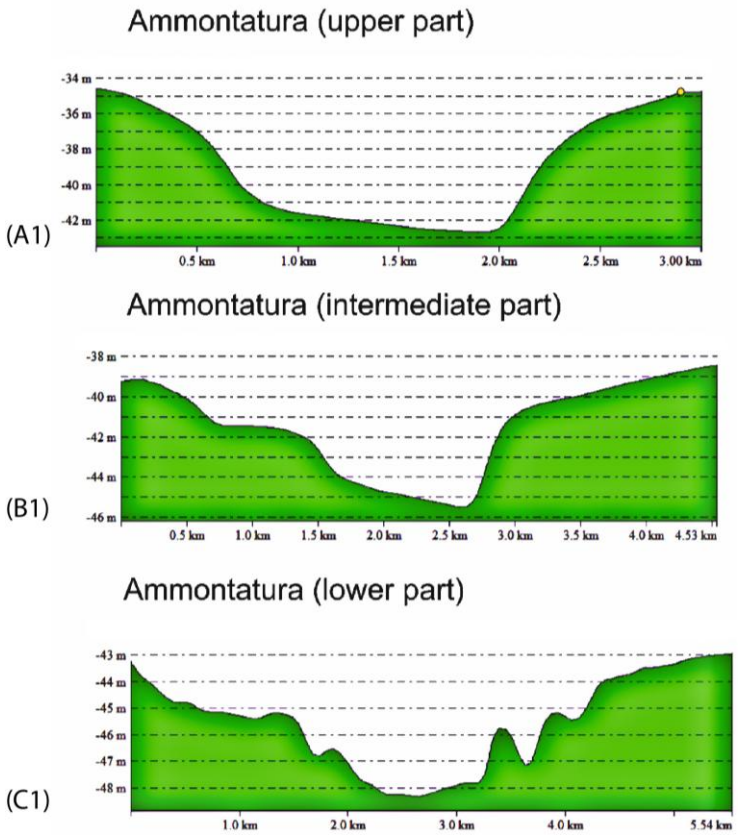
Ammontatura (upper part)
(A1)
-34 m
-36 m
-38 m
-40 m
-42 m
0.5 km
1.0 km
1.5 km
2.0 km
2.5 km
3.00 km
Ammontatura (intermediate part)
(B1)
-38 m
-40 m
-42 m
-44 m
-46 m
0.5 km
1.0 km
1.5 km
2.0 km
2.5 km
3.0 km
3.5 km
4.0 km
4.53 km
Ammontatura (lower part)
(C1)
-43 m
-44 m
-45 m
-46 m
-47 m
-48 m
1.0 km
2.0 km
3.0 km
4.0 km
5.54 km

382

Figure 9. Detailed DEM and bathymetric profiles of the Ammontatura slope basin (modified after Aiello et al. [16]).

The seismic profile GRNA35 has shown the stratigraphic architecture of the Naples Bay continental shelf (Ammontatura Channel; Figure 10), un-interpreted and interpreted seismic sections have been provided (Figures 10 and 11). The geological interpretation of the GRNA35 seismic profile showed that the Ammontatura slope basin contains two important volcanic seismic units, i.e. the Campanian Ignimbrite (CI) and the Neapolitan Yellow Tuff (NYT; Figure 11). In the two coastal and marine seismic units, Late Pleistocene and Holocene in age, volcaniclastic sedimentation is significant. The CI deposited during the isotopic stage 3, while the NYT deposited during the upper part of the isotopic stage 2, corresponding to the Transgressive System Tract (TST) in the Naples Bay. The Late Pleistocene coastal and marine deposits correspond with the TST, while the overlying Holocene coastal and marine deposits represent the Highstand System Tract (HST). The NYT seismic unit is deformed in the Banco della Montagna structure, a volcaniclastic field located in the Naples Bay continental shelf (Figures 10 and 11).

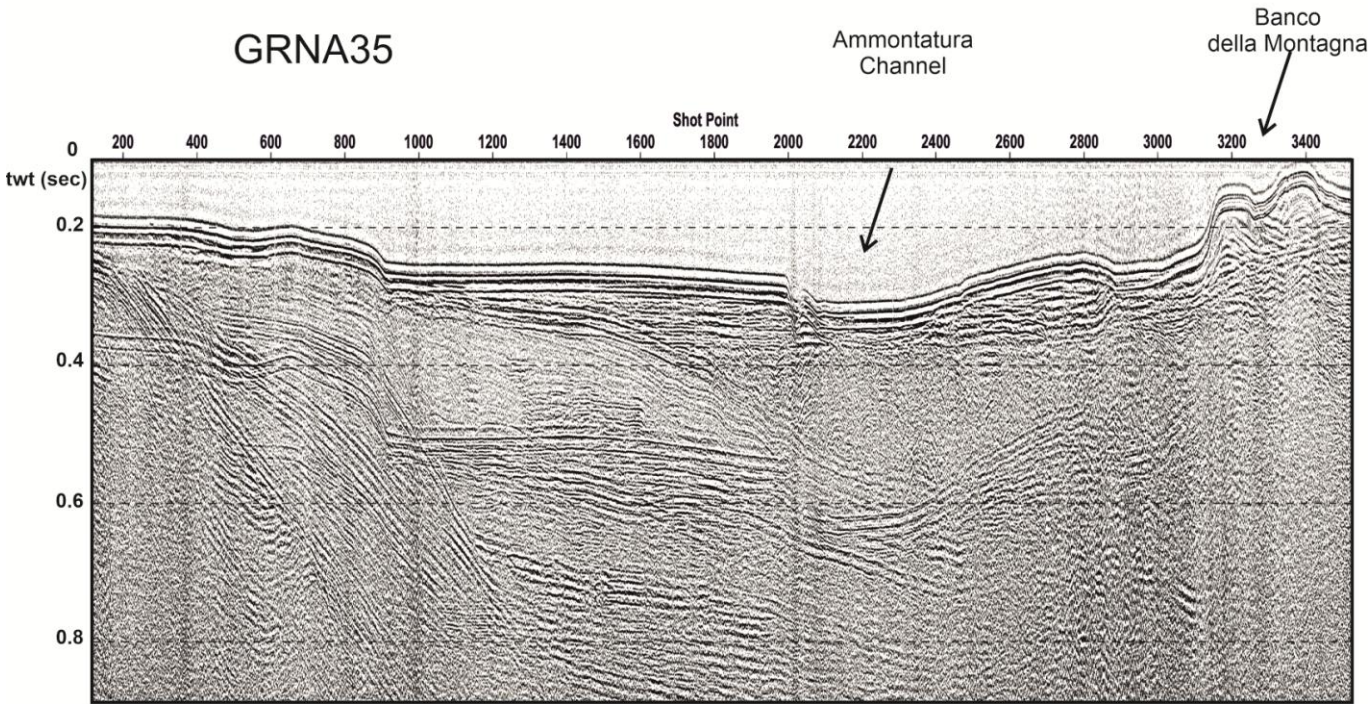

Figure 10. Seismic profile GRNA35, crossing the Ammontatura channel.

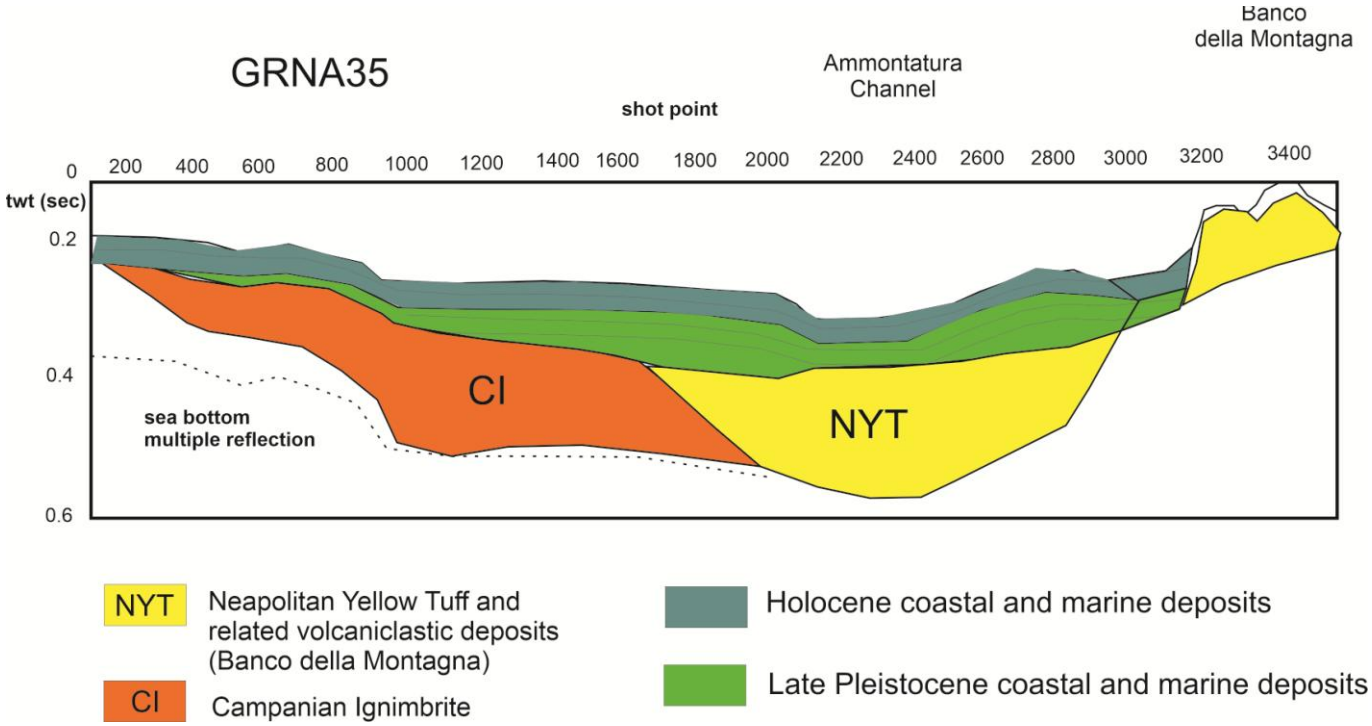

Figure 11. Geological interpretation of the seismic profile GRNA35, crossing the Ammontatura channel.

4.2.2. Northern Ischia debris avalanche deposits

The northern Ischia debris avalanche deposits are discovered in a submarine region from 20 to 180 m and include large blocks, cropping out at the seabed or fossilized by Holocene deposits. A detailed shaded relief map of the northern Ischia debris avalanche deposits is reported in Figure 12. The physiographic expression at the seabed of the northern Ischia debris avalanche deposit is represented by blocks having variable dimensions immersed in a pelitic matrix (Figure 12). The western and eastern boundary of the deposits have been identified. While the western boundary of the deposits is located next to the M.te Vico structure, the eastern one extends up the Punta La Scrofa promontory.

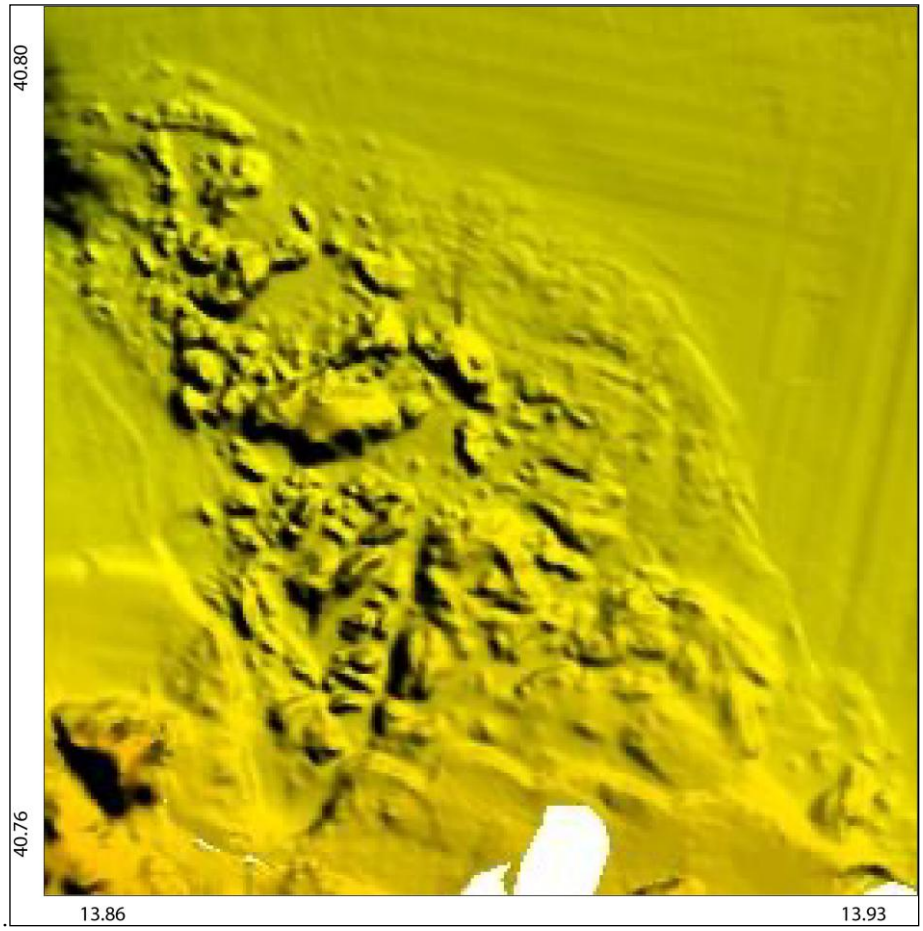

Figure 12. Detailed DEM of the northern Ischia debris avalanche.

The structure of the northern Ischia debris avalanche deposit has been studied through four bathymetric profiles (Figure 13). The first profile crossed the distal part of the deposit with a NE-SW trend. The main accumulation of the deposit rises up to the seabed to 60 m of water depth. Its sides are characterized by two channelized areas located at water depths of 110 m. The first one rises up to water depths of 100 m; the second one, wide about 4 km, reaches water depths of 90 m (Figure 13).

The second bathymetric profile crosses the northern Ischia debris avalanche deposit longitudinally with a NNW-SSE trend, at water depths ranging between 25 m and 130 m. The profile shows the irregularly articulated structure of the deposit, wide 1.8 km, with a channel bounded by levees at water depths of 55 m. Proceeding seawards, after a break in slope at 70 m, the deposit is carved by two deep channelized areas, located at water depths of 100 m. Further of them, another accumulation exists, wide 500 m, whose top reaches 70 m of water depth (Figure 13).

The third profile runs in the deposit longitudinally, with a SSW-NNE trend. For a distance of 3 km the topography of the deposit uprises to 70 m of water depth. In this area several channels occur, having variable entity and amplitude, carving the deposit. Starting from 70 m the deposit develops up to 25 m, showing two main channels along its topographic profile (Figure 13).

The fourth section has shown that the main deposit occurs at the center of the section at water depths of 60 m and is bounded by two channels, respectively located at water depths of 80 m (on the left of the deposit) and of 95 m (on the right of the deposit). Two other culminations of the deposit, respectively located at 70 m and 85 m of water depth, occur (Figure 13).

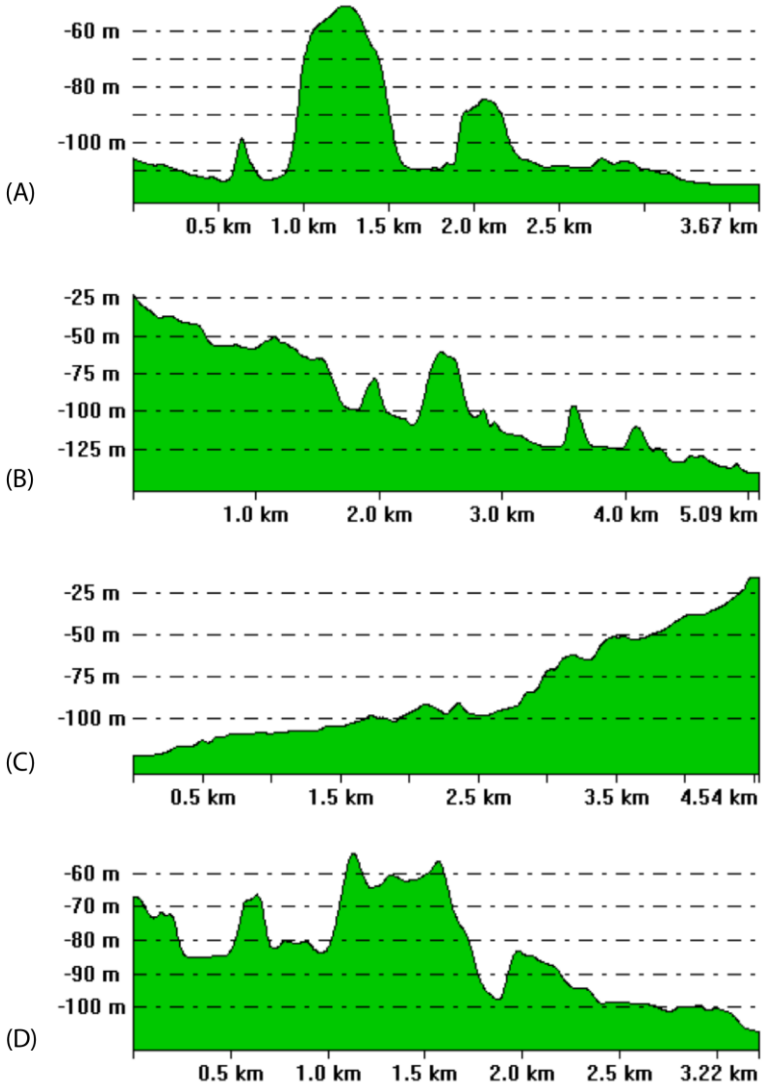

Figure 13. Bathymetric profiles in the northern Ischia debris avalanche deposits.

The northern Ischia debris avalanche deposit has been crossed by the seismic profile L27. The deposit is organized in two distinct superimposed bodies (H1 and H2; Figure 14). The basin filling is composed of three seismo-stratigraphic units (C, D, E), partly in facies hetheropy with the upper part of buried volcanic structures, acoustically-transparent and characterized by a dome-shaped external geometry (Figure 14).

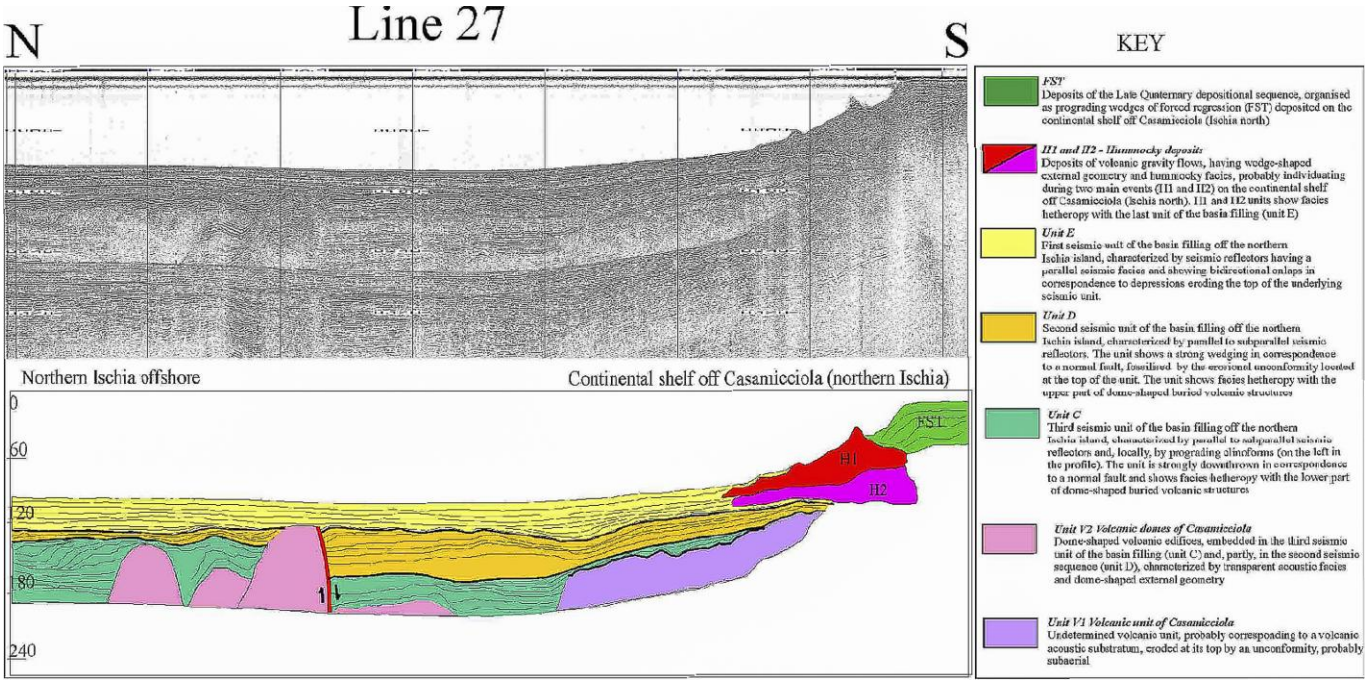

Figure 14. Seismic profile in the northern sector of Ischia (Casamicciola) and corresponding geological interpretation.

5. Discussion and conclusions

We made use of high-resolution bathymetry maps to assess the morphological pattern of the sea and establish the related marine hazard. Naples Bay is continually exposed to high-intensity human impacts that contribute to coastal zone stress and to a broad range of natural hazards, such as seismicity, volcanic activity, gravity slides, pyroclastic density currents and tsunamis. It is an area of about 900 km^2 that is part of the Campania region, which is one of the geographical regions of the world that is most vulnerable to a significant volcanic hazard, since it is a densely human-populated area. The volcanic hazard is strictly associated with the reactivation of the magmatic systems of the Phlegrean Fields, Somma-Vesuvius and Ischia Island. Ground deformation is particularly severe at the Phlegrean Fields and Ischia Island, where divergent tectonic uplift is modulated by the growth of volcano-tectonic faults and hydrothermal systems. Seismic and bradyseismic crises dominate the Phlegrean Fields, where an uplift of 1.8 m from 1982 to 1984 caused the evacuation of about 30,000 people from the town of Pozzuoli, and an actual bradyseismic crisis is still in course. Ischia has undergone, in historical times, natural seismic activity and lateral collapses. The most recent one is the Casamicciola earthquake of 2017.

Detailed marine geohazard maps of the Bay of Naples have been constructed taking into account geomorphological data and maps, previously obtained [24] (Figure 15). The obtained results have shown the suitability of the morpho-bathymetric and seismo-stratigraphic studies, when applied in studying both volcanic and sedimentary depositional environments in the Bay of Naples and that the marine hazard is higher in three districts, including the Ischia slope, the Naples canyons, and the Sorrento slope (Figure 15).

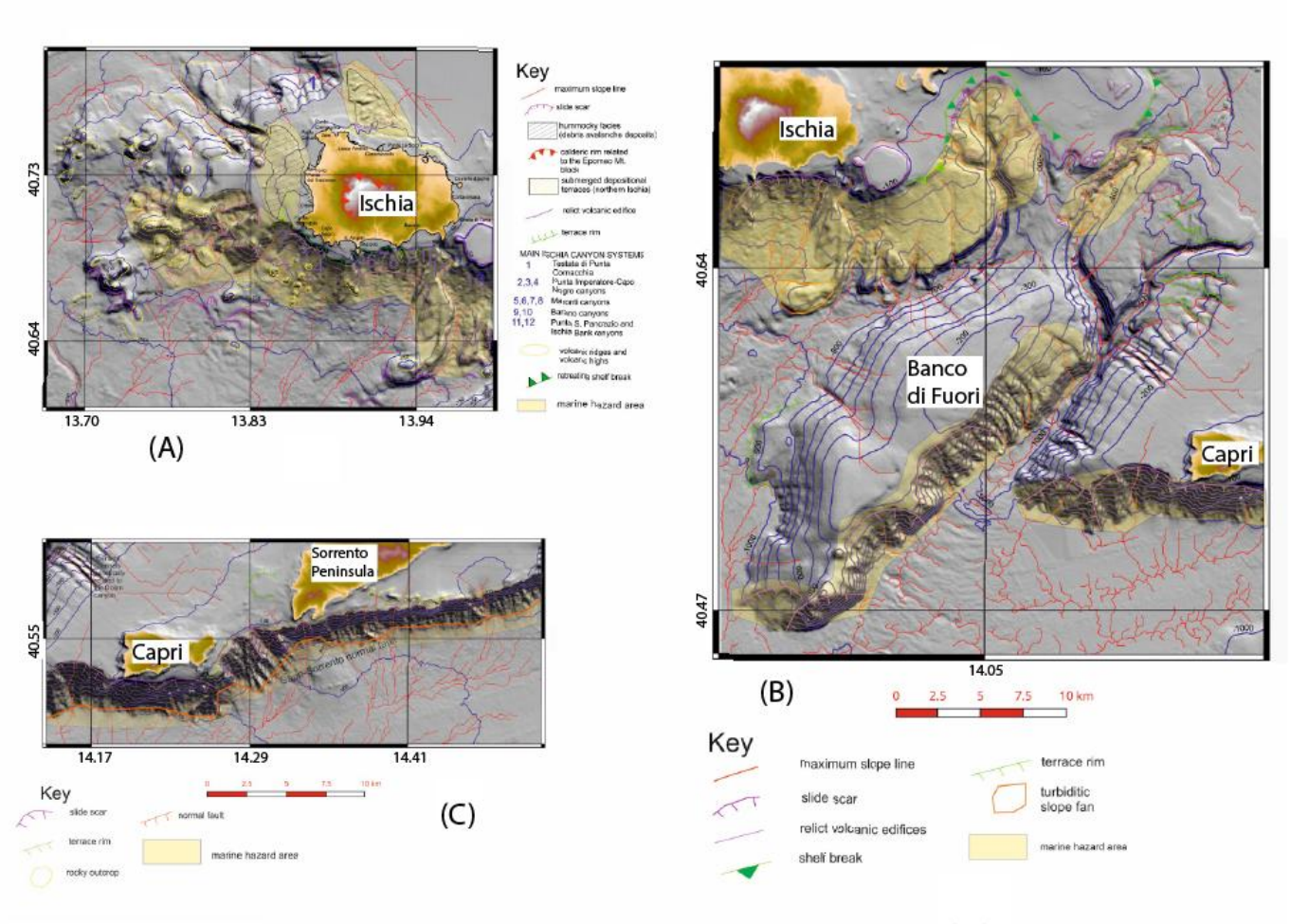

Figure 15. Detailed geomorphological maps of the Naples Bay, showing marine hazard (in yellow). (a) Ischia; (b) Naples canyons, (c) southern slope of the Sorrento Peninsula (modified after Aiello and Sacchi [24].

In the Ammontatura slope basin, the morpho-bathymetric and seismic data have shown a close relationship with the Dohrn canyon and with the important seismic units of the Naples Bay (CI and NYT; Figure 11). A significant contribution of volcaniclastic sedimentation in the Holocene marine sedimentation is suggested by sedimentological and tephrostratigraphic data on the Bay of Naples. The Ammontatura channel is a fossil branch of the Dohrn canyon, genetically related with the western branch, draining the volcaniclastic input of Campi Flegrei and Procida eruptions. The occurrence of tephra having a Phlegraean provenance in the core data [51-53] supports this work hypothesis, still in course of study. The growth of the volcanic edifice of the Nisida Bank post-dates the activity of the Ammontatura channel, abruptly ending on the volcanic edifice. The Ammontatura slope basin and related channel were active during a time interval spanning between the NYT eruption (15 ky B.P.) and the growth of the Nisida Island and Nisida Bank (4.8 - 3.7 ky B.P.).

The southern slope of the Sorrento Peninsula is a tectonically-controlled slope governed by the Capri-Sorrento normal fault. Our data have shown a dense network of drainage channels. The platform margin is incised by a dense network of drainage lines (Figure 15), which in some way, could reflect the drainage network occurring onshore, also if a physical continuity does not exist, since the channels start from the shelf break and do not continue in the narrow shelf off southern Sorrento Peninsula. These channels are the present-day and recent preferential transport routes of sediments, entering the Salerno Valley.

Offshore the Sorrento Peninsula the debris flow and stream deposits, Late Holocene in age, are composed of middle-to-fine grained pelitic sands, with abundant plant remnants and anthropic debris. Moreover, they consist of pelitic middle-to-fine-grained sands, elongated according to maximum slope lines at the seabed or as channel fillings. The depositional areas are the portions of seabed surrounding the stream mouths, along the southern slope of Sorrento Peninsula (Amalfi), oriented perpendicularly to the depositional elements of continental shelf. This lithofacies is similar to the stream deposits located at the mouth of the Bonea stream (Salerno) and has been deposited by hyper-concentrated fluxes following exceptional alluvial events, such as those of Vietri sul Mare and Maiori on 1954.

The northern Ischia Debris Avalanche deposits can be put in the frame of the eruptive activity of Ischia. A chronostratigraphic diagram of Ischia has been constructed in order to improve the discussion from the obtained data, showing also the stratigraphic relationships with the corresponding units of Procida (Figure 16).

The northern Ischia Debris Avalanche can be put in the stratigraphic framework of the 5st prehistorical cycle (0-10 ky B.P.; Figure 16). Chiocci and de Alteriis [15] explained the Southern Ischia Debris Avalanche as due to a large-scale prehistorical collapse. Della Seta et al. [38] suggested that the subaerial debris avalanches of Ischia mostly occurred since 3 ky B.P. (Figure 3, inset b). They are associated with other gravitational mass movements, including debris flows (lahars), rock falls, slumps, debris and rock slides, and small debris flows, and deep-seated gravitational slope deformation [38]. The recognition of submarine deposits genetically related with subaerial deposits highlights that the debris avalanches impacted on the sea. Based on our data we can suggest that the Northern Ischia Debris Avalanche deposits were deposited during two phases (H1 and H2) and are not associated to an evident slide scar on land, on the contrary, of the IDA [15], which is associated with a large scar of the southern flank of the island.

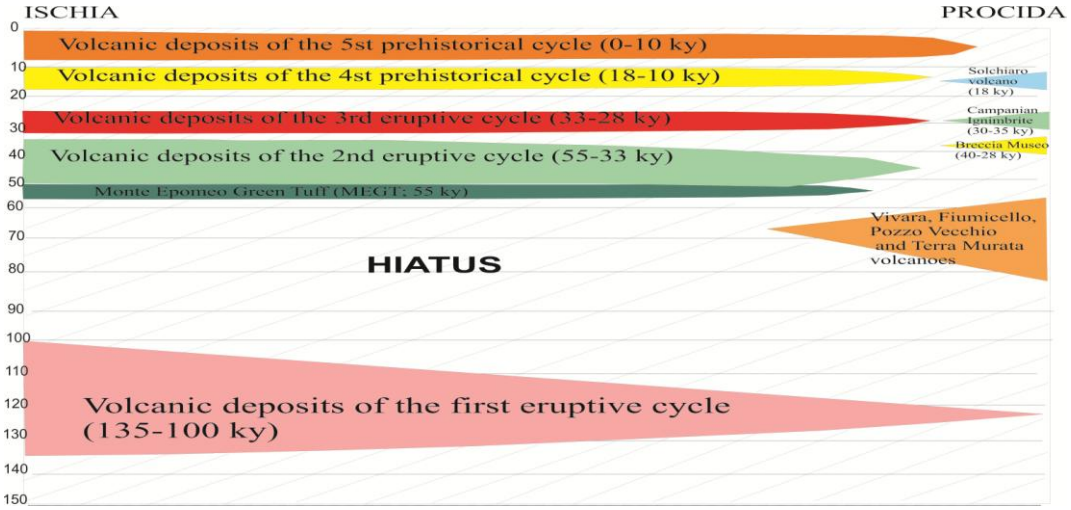

Figure 16. Qualitative chronostratigraphic diagram of Ischia.

Author Contributions: formal analysis, G.A and M.C..; investigation, G.A.; writing—original draft preparation, G.A.; writing—review and editing, G.A.. All authors have read and agreed to the published version of the manuscript.

Funding: This research received no external funding.

Conflicts of Interest: The authors declare no conflicts of interest.

References

1. Kopp, H.; Chiocci, F. L.; Berndt, C.; Çağatay, M. N.; Ferreira, T.; Fortes, C. J. E. M.; Gràcia, E.; González Vega, A.; Kopf, A.; Sørensen, J.; Sultan, M. B.; Yeo, I. A. *Marine geohazards: Safeguarding society and the Blue Economy from a hidden threat.* Position

Paper 26 of the European Marine Board, 2021, Ostend, Belgium, pp. 1-100. ISSN: 2593-5232. ISBN: 9789464206111 DOI: 10.5281/zenodo.5591938.

2. International Centre for Geohazard (2003). Offshore Geohazards. https://www.ngi.no/eng/Projects/ICGInternational-Centre-for-Geohazards/OffshoreGeohazards.
3. CIESM *Marine geo-hazards in the Mediterranean*. CIESM Workshop Monographs, 2011, Monaco, 42, pp. 1-192.
4. Urgeles, R.; Camerlenghi, A. Submarine landslides of the Mediterranean Sea: Trigger mechanisms, dynamics, and frequency-magnitude distribution. *Journ. Geophys. Res*., **2013**, *118*, 2600–2618, doi:10.1002/2013JF002720.
5. Ceramicola, S.; Praeg, D.; Coste, M.; Forlin, E.; Cova, A.; Colizza E., Critelli S. Submarine Mass-Movements Along the Slopes of the Active Ionian Continental Margins and Their Consequences for Marine Geohazards (Mediterranean Sea). In *Submarine Mass Movements and Their Consequences*, 1st Ed., Krastel, S., Behrmann, J., Volker, G., Urgeles, R., Chaytor, J., Huhn, K, Strasser, N., Harbitz, C., Eds., Advances in Natural and Technological Hazards Research, Springer: Cham, Switzerlad, 2014, volume 37, pp. 295-306, https://doi.org/10.1007/978-3-319-00972-8_26.
6. Camargo J.M.R., Silva M., Ferreira A., Araujio T. (2019) Marine Geohazards: A Bibliometric-Based Review. *Geosciences* **2019**, *9*, 100, doi:10.3390/geosciences9020100.
7. Chivata Cardenas, I.; Flage, R.; Aven, T. Marine geohazards exposed: Uncertainties involved. *Marine Georesources and Geotechnology*, **2023**, *41*, 6, 589-619, https://doi.org/10.1080/1064119X.2022.2078252.
8. Wang, Y., Heidarzadeh, M., Satake, K., Mulia, I. E., Yamada, M. A tsunami warning system based on offshore bottom pressure gauges and data assimilation for Crete Island in the Eastern Mediterranean Basin. *Journal of Geophysical Research* Solid Earth **2020**, *125*, e2020JB020293. https://doi.org/10.1029/2020JB020293.
9. Heidarzadeh M., Gusman A.R., Mulya I.R., The landslide source of the eastern Mediterranean tsunami on 6 February 2023 following the Mw 7.8 Kahramanmaraş (Türkiye) inland earthquake. *Geoscience Letters* **2023**, *10*, 50 https://doi.org/10.1186/s40562-023-00304-8.
10. Fusi, N.; Mirabile, L.; Camerlenghi, A.; Ranieri, G. Marine geophysical survey of the Gulf of Naples (Italy): Relationship between submarine volcanic activity and sedimentation. *Mem. Soc. Geol. Ital.* **1991**, *47*, 95–114.
11. Milia, A.; Torrente, M.; Russo, M.; Zuppetta, A. Tectonics and crustal structure of the Campania continental margin: relationships with volcanism. *Mineralogy and Petrology* **2003**, *79*, 33–47. https://doi.org/10.1007/s00710-003-0005-5.,
12. Insinga, D.; Molisso, F.; Lubritto, C.; Sacchi, M.; Passariello, I.; Morra, V. The proximal marine record of Somma–Vesuvius volcanic activity in the Naples and Salerno bays, Eastern Tyrrhenian Sea, during the last 3 kyrs. *Journ. of Volcanol. and Geoth. Res.* **2008**, *177* (1), 170-186, https://doi.org/10.1016/j.jvolgeores.2007.07.011.
13. Sacchi, M.; Pepe, F.; Corradino, M.; Insinga, D.D.; Molisso, F.; Lubritto, C. The Neapolitan Yellow Tuff caldera offshore the Campi Flegrei: Stratal architecture and kinematic reconstruction during the last 15 ky. *Marine Geology* **2014**, *354*, 15-33.
14. Sacchi, M.; De Natale, G.; Spiess, V.; Steinmann, L.; Acocella, V. ; Corradino, M.; de Silva, S.; Fedele, A.; Fedele, L.; Geshi, N.; Kilburn, C.; Insinga, D.; Jurado, M.; Molisso, F.; Petrosino, P.; Passaro, S.; Pepe, F.; Porfido, S.; Scarpati, C.; Schmincke, H.; Somma, R.; Sumita, R.; Tamburrino, S.; Troise, C.; Vallefuoco, M.; Ventura, G. A roadmap for amphibious drilling at the Campi Flegrei caldera: insights from a MagellanPlus workshop. *Scientific Drilling* **2019**, *26*, 29–46, https://doi.org/10.5194/sd-26-29-2019.
15. Chiocci, F.L.; De Alteriis, G The Ischia debris avalanche: first clear submarine evidence in the Mediterranean of a volcanic island prehistorical collapse. *Terra Nova* **2006**, *18* (3), 202-209, https://doi.org/10.1111/j.1365-3121.2006.00680.x.
16. de Alteriis, G., Scotto di Santolo, A., Chiocci, F.L., Ramondini, M., Violante, C. The Case of Ischia Underwater Debris Avalanche (Italy, Tyrrhenian Sea) and Its High Mobility. In: Lollino, G., Manconi, A., Locat, J., Huang, Y., Canals Artigas, M. (Eds) *Engineering Geology for Society and Territory* – Volume 4. Springer, Cham, 2014, https://doi.org/10.1007/978-3-319-08660-6_43
17. Milia, A. The Dohrn canyon: A response to the eustatic fall and tectonic uplift of the outer shelf along the eastern Tyrrhenian sea margin, Italy. *Geo-Mar. Lett.* **2000**, *20*, 101–108.
18. Aiello, G.; Iorio, M.; Molisso, F.; Sacchi, M Integrated Morpho-Bathymetric, Seismic-Stratigraphic, and Sedimentological Data on the Dohrn Canyon (Naples Bay, Southern Tyrrhenian Sea): Relationships with Volcanism and Tectonics. *Geosciences* **2020**, 10, 319. https://doi.org/10.3390/geosciences10080319.
19. Tinti, S.; Pagnoni, G.; Piatanesi, A. Simulation of tsunamis induced by volcanic activity in the Gulf of Naples (Italy). *Nat Hazards Earth Syst Sci* **2003**, *3*, 311–320.
20. Tinti, S.; Chiocci, F.L.; Zaniboni, F.; Pagnoni, G.; de Alteriis, G. Numerical simulation of the tsunami generated by a past catastrophic landslide on the volcanic island of Ischia, Italy. *Marine Geophysical Research* **2011**, *32*, 287–297. https://doi.org/10.1007/s11001-010-9109-6.
21. Selva, J.; Acocella, V.; Bisson, M.; Caliro, S.; Costa, A.; Della Seta, M.; De Martino, P.; de Vita, S.; Giordano, G.; Martino, S.; Cardaci, C. Multiple natural hazards at volcanic islands: a review for the Ischia volcano (Italy). *Journal of Applied Volcanology* **2019**, *8*, 5, https://doi.org/10.1186/s13617-019-0086-4.
22. Grezio, A.; Cinti, F. R.; Costa, A.; Faenza, L.; Perfetti, P.; Pierdominici, S.; Grezio, A.; Cinti, F. R.; Costa, A.; Faenza, L.; Perfetti, P.; Pierdominici, S.; Pondrelli, S.; Sandri, L.; Tierz, P.; Tonini, L. Multisource Bayesian probabilistic tsunami hazard analysis for the Gulf of Naples (Italy). *Journal of Geophysical Research*, **2020** 125, e2019JC015373. https://doi.org/10.1029/2019JC015373.
23. Aiello, G.; Caccavale, M. Quaternary Evolution of Ischia: A Review of Volcanology and Geology. *Appl. Sci.* **2023**, *13*, 3554. https://doi.org/10.3390/app13063554.

24. Aiello, G.; Sacchi, M. New morpho-bathymetric data on marine hazard in the offshore of Gulf of Naples (Southern Italy). *Natural Hazards* **2022**, *111*, 2881–2908, https://doi.org/10.1007/s11069-021-05161-2.
25. Patacca, E.; Scandone, P. Geology of Southern Apennines. *Boll. Soc. Geol. Ital.* **2007**, *Spec. Issue No. 7*, 75-119.
26. Milia, A.; Torrente, M.M. Tectonics and stratigraphic architecture of a peri-Tyrrhenian half-graben (Gulf of Naples, Italy). *Tectonophysics* **1999**, *315* (1), 301–318. DOI: 10.1016/S0040-1951(99)00280-2.
27. Conti, A.; Bigi, S.; Cuffaro, M.; Doglioni, C.; Scrocca, D.; Muccini, F.; Cocchi, L.; Ligi, M.; Bortoluzzi, G. Transfer zones in an oblique back-arc basin setting: Insights from the Latium-Campania segmented margin (Tyrrhenian Sea). *Tectonics* **2017**, *36*, 78–107.
28. Malinverno, A. Evolution of the Tyrrhenian Sea-Calabrian Arc system: The past and the present. *Rend Online Soc. Geol. Ital.* **2012**, *21*, 11-15.
29. Bigi, G.; Coli, M.; Cosentino, D.; Dal Piaz, G. V.; Parotto, M.; Sartori, R.; Scandone, P. *Structural Model of Italy – scale 1: 500.000.* CNR 1983- SELCA 1992.
30. Vitale, S.; Ciarcia, S. Tectono-stratigraphic setting of the Campania region (southern Italy). *Journ. of Maps* **2018**, *14* (2), 9-21. DOI: 10.1080/17445647.2018.1424655.
31. Iannace, A.; Merola, D.; Perrone, V.; Amato, A.; Cinque, A.; Santacroce, R.; Sbrana, A.; Sulpizio, R.; Zanchetta, G.; Budillon, F.; D'Argenio, B.; Conforti, A. (2015) *Note illustrative della carta geologica d'Italia alla scala 1: 50.000 – Fogli 466 – 485 "Sorrento-Termini".* ISPRA, Servizio Geologico d'Italia, pp. 1-201. Available from: https://www.isprambiente.gov.it/Media/carg/note_illustrative/466_485_Sorrento_Termini.pdf [Accessed: 2024-2-26].
32. Gurioli, L.; Sulpizio, R.; Cioni, R.; Sbrana, A.; Santacroce, R.; Luperini, W.; Andronico, D. Pyroclastic flow hazard assessment at Somma–Vesuvius based on the geological record. *Bull. of Volcanol.* **2010**, *72*, 1021–1038, DOI: 10.1007/s00445-010-0379-2.
33. Bruno, P.; de Alteriis, G.; Florio, G. The western undersea section of the Ischia volcanic complex (Italy, Tyrrhenian sea) inferred by marine geophysical data. *Geophys. Res. Lett.* **2002**, *29*, 9. DOI:10.1029/2001GL013904.
34. De Vita, S.; Sansivero, F.; Orsi, G.; Marotta, E., Cyclical slope instability andvolcanism related to volcano-tectonism in resurgent calderas: the Ischia island(Italy) case study. *Eng. Geol.* **2006**, 86, 148–165.
35. De Alteriis, G.; Violante, C. Catastrophic landslides off Ischia volcanic island (Italy) during prehistory. In: Violante, C. (Ed.) *Geohazard in Rocky Coastal Areas*. The Geological Society, London, Special Publications, 2009 322, 73–104. DOI: 10.1144/SP322.3.
36. Sbrana, A.; Toccaceli, R. M.; Biagio, G.; Cubellis, E.; Faccenna, C.; Fedi, M.; Florio, G.; Fulignati, P.; Giordano, F.; Giudetti, G.; Grimaldi, M.; Italiano, F.; Luperini, W.; Marianelli, P.;, Buia, M. C.; Donadio, C.; Gambi, M. C.; Putignano, M. L.; Aiello, G.; Budillon, F.; Conforti, A.; D'Argenio, B. (2011) *Geologic map of Ischia, scale 1:10.000 – maps and explanatory notes.* Campania Region, Sector of Soil Defence, Geothermics and Geotechnics, Naples, Italy
37. Sbrana, A.; Marianelli, P.; Pasquini, G. Volcanology of Ischia (Italy). *Journ. of Maps* **2018**, 14 (2), 494-503, DOI: 10.1080/17445647.2018.1498811.
38. Della Seta, M.; Marotta, E.; Orsi, G.; De Vita, S.; Sansivero, F.; Fredi, P. Slope instability induced by volcano-tectonics as an additional source of hazard in active volcanic areas: the case of Ischia island (Italy). *Bull. of Volcanol.* **2012**, *74* (1), 79-106. DOI 10.1007/ s00445-011-0501-0.
39. Kilburn, C.R.J.; Carlino, S.; Danesi, S.; Pino, N.A. Potential for rupture before eruption at Campi Flegrei caldera, Southern Italy. *Communications Earth and Environment* **2023**, *4*, 190, https://doi.org/10.1038/s43247-023-00842-1.
40. De Novellis, V.; Carlino, S.; Castaldo, R.; Tramelli, A.; De Luca, C.; Pino, N. A.; Pepe, S.; Convertito, V.; Zinno, I.; De Martino, P.; Bonano, M.; Giudicepietro, F.; Casu, F.; Macedonio, G.; Manunta, M.; Cardaci, C.; Manzo, M.; Di Bucci, D.; Solaro, G.; Zeni, G.; Lanari, R.; Bianco, F.; Tizzani, P. The 21 August 2017 Ischia (Italy) earthquake source model inferred from seismological, GPS, and DInSAR measurements. *Geophys Res Lett* **2018**, *45*, 2193–2202. https://doi.org/10.1002/2017GL076336.
41. Di Fiore, V.; Aiello, G.; D'Argenio, B. Gravity instabilities in the Dohrn Canyon (Bay of Naples, Southern Tyrrhenian Sea): Potential wave and run-up (tsunami) reconstruction from a fossil submarine landslide. *Geol. Carpathica* **2011**, *62*, 55–63.
42. Pratson, L.F.; Coakley, B.J. A model for the headward erosion of submarine canyons induced by downslope-eroding sediment flows. *Geol. Soc. Am. Bull.* **1996**, *108*, 225–234.
43. Aiello, G.; Caccavale, M. The Coastal Areas of the Bay of Naples: The Sedimentary Dynamics and Geological Evolution of the Naples Canyons. *Geosciences* **2023**, *13*, 226, https://doi.org/10.3390/geosciences13080226.
44. Satow, C.; Watt, S.; Cassidy M.; Pyle, D.; Deng, Y.N. The Contributions of Marine Sediment Cores to Volcanic Hazard Assessments: Present Examples and Future Perspectives. *Geosciences* **2023**, *13*, 124. https://doi.org/10.3390/geosciences13040124.
45. Brown, R.J.; Orsi, G.; De Vita, S. New insights into Late Pleistocene explosive volcanic activity and caldera formation on Ischia (southern Italy). *Bull. Volcanol*. **2008**, *70*, 583–603.
46. de Alteriis, G.; Insinga, D.D. ; Morabito, S. ; Morra, V.; Chiocci, F.L. ; Terrasi, F. ; Lubritto, C. ; Di Benedetto, C. ; Pazzanese, M. Age of submarine debris avalanches and tephrostratigraphy offshore Ischia Island, Tyrrhenian Sea, Italy. *Marine Geology* **2010**, *278*, 1–4, , 1-18, https://doi.org/10.1016/j.margeo.2010.08.004.
47. de Vita, S.; Di Vito, M.A.; Gialanella, C.; Sansivero, F. The impact of the Ischia Porto Tephra eruption (Italy) on the Greek colony of Pithekoussai, *Quaternary International* **2013**, *303*, 142-152, https://doi.org/10.1016/j.quaint.2013.01.002.
48. Tomlinson, E.; Albert, P.G.; Wulf, S.; Brown, R.J.; Smith, V.C.; Keller, J.; Orsi, G.; Bourne, A.J.; Menzies, M. A. (2014) Age and geochemistry of tephra layers from Ischia, Italy: constraints from proximal-distal correlations with Lago Grande di Monticchio. *Journ. of Volcanol. and Geoth. Res.* **2014**, *287*, 22-39, https://doi.org/10.1016/j.jvolgeores.2014.09.006.

49. D'Antonio, M.; Arienzo, I.; Brown, R.J.; Petrosino, P.; Pelullo, C.; Giaccio, B. Petrography and Mineral Chemistry of Monte Epomeo Green Tuff, Ischia Island, South Italy: Constraints for Identification of the Y-7 Tephrostratigraphic Marker in Distal Sequences of the Central Mediterranean. *Minerals* **2021**, *11*, 955. https://doi.org/10.3390/min11090955.
50. Primerano, P.; Giordano, G.; Costa, A.; de Vita, S.; Di Vito, M.A. Reconstructing fallout features and dispersal of Cretaio Tephra (Ischia Island, Italy) through field data analysis and numerical modelling: Implications for hazard assessment. *Journ. of Volcanol. and Geotherm. Res.* **2021**, *415*, 107248.63.
51. Sacchi, M.; Insinga, D.; Milia, A.; Molisso, F.; Raspini, A.; Torrente, M.M.; Conforti, A. Stratigraphic signature of the Vesuvius 79 AD event off the Sarno prodelta system, Naples Bay. *Marine Geology* **2005**, *222–223*, 443–469.
52. Insinga, D.D.; Petrosino, P.; Alberico, I.; de Lange, G.J.; Lubritto, C.; Molisso, F.; Sacchi, M.; Sulpizio, R.; Wu, J.; Lirer, F. (2020) The Late Holocene tephra record of the central Mediterranean Sea: Mapping occurrences and new potential isochrons for the 4.4–2.0 ka time interval. *Journal of Quaternary Sciences*, 35, 213-231. https://doi.org/10.1002/jqs.3154.
53. Sacchi, M.; Passaro, S.; Molisso, F.; Matano, F.; Steinmann, L.; Spiess, V.; Pepe, F.; Corradino, M.; Caccavale, M.; Tamburrino, S.; et al. The Holocene marine record of unrest, volcanism, and hydrothermal activity of Campi Flegrei and Somma Vesuvius. In *Vesuvius, Campi Flegrei, and Campanian Volcanism*, De Vivo, B., Belkin, H.E., Rolandi, G., Eds.; Elsevier Inc.: Amsterdam, The Netherlands, 2020; pp. 435–469.
54. de Vita, S.; Sansivero, F.; Orsi, G.; Marotta, E.; Piochi, M. Volcanological and structural evolution of the Ischia resurgent caldera (Italy) over the past 10 ka. In *Stratigraphy and geology of volcanic areas*, Groppelli, G., Viereck, L., eds., GSA book series, Special paper 464; 2010. pp. 193–239.
55. Alberico, I.; Lirer, L.; Petrosino, P.; Scandone, R. Volcanic hazard and risk assessment from pyroclastic flows at Ischia Island (southern Italy). *Journ. of Volcanol. and Geotherm Res.* **2008**, *171*, 118–136.
56. Gurioli, L.; Cioni, R.; Sbrana, A.; Zanella, E. Transport and deposition of pyroclastic density currents over an inhabited area: the deposits of the AD 79 eruption of Vesuvius at Herculaneum (Italy). *Sedimentology* **2002**, *49*, 929-953.
57. Cioni, R.; Gurioli, L.; Lanza, R.; Zanella, E. Temperatures of the A.D. 79 pyroclastic density current deposits (Vesuvius, Italy). *Journal of Geophysical Research* **2004**, *109*, B02207, doi: 10.1029/2002JB002251.
58. Gurioli, L.; Zanella, E.; Pareschi, M. T.; Lanza, R Influences of urban fabric on pyroclastic density currents at Pompeii (Italy) I: flow direction and deposition. *Journal of Geophysical Research* **2007**, *112*, B05213, doi: 10.1029/2006JB004444.
59. Shea, T.; Gurioli, L.; Houghton, B. F.; Cioni, R.; Cashman, K. V. Column collapse and generation of pyroclastic density currents during the A.D. 79 eruption of Vesuvius: The role of pyroclastic density. *Geology* **2011**, *39* (7), 695-698, doi: 10.1130/G32092.1.
60. Cioni, R.; Tadini, A.; Gurioli, L.; Bertagnini, A.; Mulas, M.; Bevilacqua, A.; Neri, A. Estimating eruptive parameters and related uncertainties for pyroclastic density current deposits: worked examples from Somma-Vesuvius (Italy). *Bull. of Volcanol.* **2020**, Springer Verlag, 2020, 82 (9), ff10.1007/s00445-020-01402-7ff. ffhal-03001964.
61. Tadini, A.; Bevilacqua, A.; Neri, A.; Cioni, R.; Biagioli, G.; Vitturi, M.; Esposti Ongaro, T. Reproducing pyroclastic density current deposits of the 79 CE eruption of the Somma-Vesuvius volcano using the box-model approach. *Solid Earth* **2021**, *12*, 119-139, https://doi.org/10.5194/se-12-119-2021. 74.
62. Aiello, G. Submarine Stratigraphy of the Eastern Bay of Naples: New Seismo-Stratigraphic Data and Implications for the Somma-Vesuvius and Campi Flegrei Volcanic Activity. *Journ. of Marine Science Engineering* **2022**, *10*, 1520. https://doi.org/10.3390/jmse10101520.
63. Milia, A.; Molisso, F.; Raspini, A.; Sacchi, M.; Torrente, M.M. Syneruptive features and sedimentary processes associated with pyroclastic currents entering the sea: the AD 79 eruption of Vesuvius, Bay of Naples, Italy. *Journal of the Geological Society of London* **2008**, *165*, 839–848.
64. Sparks, R.S.J.; Sigurdsson, H.; Carey, S.N. (1980) The entrance of pyroclastic flows into the sea, II. Theoretical considerations on subaqueous emplacement and welding. *Journ. of Volcanol. and Geoth. Res.* **1980**, 7 (1–2), 97-105, https://doi.org/10.1016/0377-0273(80)90022-0.77.
65. Trofimovs, J.; Sparks, R.S.J.; Talling, P.J. Anatomy of a submarine pyroclastic flow and associated turbidity current: July 2003 dome collapse, Soufrière Hills volcano, Montserrat, West Indies. *Sedimentology* **2008**, *55*, 617-634. https://doi.org/10.1111/j.1365-3091.2007.00914.x.
66. Di Capua, A.; Groppelli, G. Emplacement of pyroclastic density currents (PDCs) in a deep-sea environment: The Val d'Aveto Formation case (Northern Apennines, Italy). *Journ. of Volcanol. and Geoth. Res.* **2016**, *328*, 1-8. https://doi.org/10.1016/j.jvolgeores.2016.08.003.
67. Clare, M.A. et al. Fast and destructive density currents created by ocean-entering volcanic eruptions. *Science* **2023**, *381*, 1085-1092.DOI:10.1126/science.adi3038.
68. Maeno F., Imamura F. Tsunami generation by a rapid entrance of pyroclastic flow into the sea during the 1883 Krakatau eruption, Indonesia. *Journ. of Geophysical Research* **2011**, *116*, B09205, doi:10.1029/2011JB008253.
69. Alberico, I.; Di Fiore, V.; Iavarone, R.; Petrosino, P.; Piemontese, L.; Tarallo, D.; Punzo, M.; Marsella, E. (2015) The Tsunami Vulnerability Assessment of Urban Environments through Freely Available Datasets: The Case Study of Napoli City (Southern Italy. *Journ. of Marine Science and Engineering* 2015, 3, 981-1005; doi:10.3390/jmse3030981.
70. Paris, R.; Ulvrova, M.; Selva, J.; Brizuela, B.; Costa, A.; Grezio, A.; Lorito, S.; Tonini R. Probabilistic hazard analysis for tsunamis generated by subaqueous volcanic explosions in the Campi Flegrei caldera, Italy. *Journ. of Volcanol. and Geothermal Res.* **2019**, *379*, 106-116, https://doi.org/10.1016/j.jvolgeores.2019.05.010.

711 71. Rosi, M.; Levi, S. T.; Pistolesi, M.; Bertagnini, A.; Brunelli, D.; Cannavò, V.; Di Renzoni, A.; Ferranti, F.; Renzulli, A.; Yoon, D.
712 Geoarchaeological Evidence of Middle-Age Tsunamis at Stromboli and Consequences for the Tsunami Hazard in the Southern
713 Tyrrhenian Sea. *Scientific Reports* **2019**, *9* (1), 677. doi:10.1038/s41598-018-37050-3.
714 72. Maramai, A.; Graziani, L.; Brizuela, B. Italian Tsunami Effects Database (ITED): The First Database of Tsunami Effects Ob-
715 served Along the Italian Coasts. *Frontiers in Earth Science* **2021**, 9, 596044. https://doi.org/10.3389/feart.2021.596044.
716 73. Tateo, F. (2010). Horribile dictu: environmental catastrophes and writing in the late Middle Ages. In Mattheus M. (ed.). Le ca-
717 lamità ambientali nel tardo Medioevo europeo: realtà, percezioni, reazioni : atti del XII Convegno del Centro studi sulla civiltà
718 del tardo Medioevo : S. Miniato, 31 maggio-2 giugno 2008. Centro studi sulla civiltà del Tardo Med (in Italian). Vol. 12. Firenze
719 University Press. p. 111. ISBN 978-88-8453-499-6. Retrieved 21 June 2012.
720

721